Electronic Supplementary Material (ESI) for Green Chemistry.

Supplementary Information

Solvent-base mismatch enables the deconstruction of epoxy polymers and bisphenol A recovery

Hongwei Sun[1], Alexander Ahrens*[1], Gabriel Martins Ferreira Batista[1], Bjarke S. Donslund[1], Anne K. Ravn[1], Emil Vincent Schwibinger[1], Ainara Nova Flores[2], Troels Skrydstrup*[1]

[1]Carbon Dioxide Activation Center (CADIAC), Novo Nordisk Foundation CO_2 Research Center, Department of Chemistry and Interdisciplinary Nanoscience Center (iNANO), Aarhus University, Gustav Wieds Vej 14, 8000 Aarhus C, Denmark.

[2]Department of Chemistry, Hylleraas Centre for Quantum Molecular Sciences and Centre for Materials Science and Nanotechnology, University of Oslo, N-0315 Oslo, Norway.

*Corresponding author. Email: aahrens@inano.au.dk, ts@chem.au.dk

Contents

1. General Information

Unless stated otherwise, all reactions were set up in a glovebox under an atmosphere of argon. All chemicals were purchased from Sigma-Aldrich, Tokyo Chemical Industry (TCI), VWR Chemicals or Strem Chemicals and used as received unless stated otherwise. NaOH (98.6% purity) was purchase from VWR Chemicals as pellets and crushed in a mortar, yielding a powder. THF, toluene, CH_2Cl_2 and MeCN were retrieved from a MBraun SP-800 purification system, degassed using argon and stored over 3 Å molecular sieves. The remaining solvents were purchased from Sigma-Aldrich degassed using argon, stored over 3 Å molecular sieves and used without further purification. Water content of solvents were tested with Coulometric KF Titrator (Mettler Toledo C20. Specifically anhydrous toluene and commercially available toluene used in this manuscript were tested as 5.9 ppm and 308.6 ppm.

Thin layer chromatography (TLC) was carried out on pre-coated aluminium sheets ALUGRAM® Xtra SIL G/UV254 purchased by Macherey-Nagel. Visualisation of the products was achieved by UV-light irradiation (366 nm) and / or staining with a potassium permanganate in water.

Flash column chromatography was carried out using Silica gel (0.040 – 0.063 mm/ 230 – 400 mesh) ASTM purchased from Macherey-Nagel. Automated flash column chromatography (AFCC) was carried out with Interchim PuriFlash XS520Plus with 30 µm prepacked columns. Celite®545, coarse, was used for filtration.

Gas chromatography - mass spectrometry (GC-MS) were measured with an Agilent 8890 gas chromatograph coupled with an Agilent 5977B mass selective detector.

High resolution mass spectrometry (HRMS): ESI(+) spectral analysis were measured with a Bruker Maxis Impact Spectrometer. MALDI spectral analysis were measured on a Bruker Autoflex maX MALDI-TOF MS spectrometer using a MTP 384 target plate polished steel BC.

Nuclear Magnetic Resonance spectroscopy: ^{1}H NMR and ^{13}C NMR spectra were recorded on a Bruker 400 MHz Ascend spectrometers. Chemical shifts were given as δ value (ppm) with reference to residual solvent signal of the deuterated solvent. The peak patterns are indicated as follows: s, singlet; d, doublet; t, triplet; m, multiplet; q, quartet. Multiplicities reported for ^{13}C NMR spectra were assigned using DEPT-90 and/or DEPT-135 spectra. The coupling constants, *J*, are reported in Hertz (Hz). The spectra were calibrated to the residual solvent signals. NMR spectra were processed with MestReNova Version 14.2.1-27684.

Particle size distributions were determined using a Malvern Mastersizer 2000 instrument with a Hydro S dispersion unit. The measurements were performed by means of laser diffraction and particles in the size interval from 0.02-2000 µm were measured. The sample was measured with constant stirring to avoid sedimentation according to ISO13320:2020 using a stirring rate of 3500 rpm and laser wavelengths of 633 nm and 466 nm. A refractive index of 1.5 and an absorption of 0.1 was assumed for the size distribution modelling of a sample of spherical particles. The result is reported as an average of triplicate measurement.

Reaction set up: All deconstruction reactions in small scale were set up in an Argon charged glovebox using a 10 ml or 40 ml COtubes sealed with PTFE/silicon seals purchased from SyTracks as reaction vessel, a Teflon-coated stirring bar with dried and degassed solvents. Reactions were stirred in metal heating blocks at 800 rpm for soluble compounds or at 300 rpm for powdered resin.

Reaction set up: Reactions were set up in an Argon charged glovebox using a 10 ml or 40 ml COtubes sealed with PTFE/silicon seals purchased from SyTracks as reaction vessel, a Teflon-coated stirring bar with dried and degassed solvents. Reactions were stirred in metal heating blocks at 650 rpm. **Warning: Glassware under pressure.**

- glass equipment should always be examined for damages to its surface, which may weaken its strength

- one must abide to all laboratory safety procedures and always work behind a shield when working with glass equipment under pressure
- COware is pressure tested to 224 psi but should under no circumstances be operated above 60 psi (5 bar)

Fig. S1. 10 ml COtube with screw cap, Teflon disc and septum.

Reactions using 1.00 g of starting material were set up in 45 mL high pressure reactor using a 30 mL PTFE inlay purchased from Parr Instrument Company.

Figure S2. 45 mL steel autoclave with 30 mL PTFE inlay.

Samples of polymeric materials: The L-Cystine containing resin (Fig. 4) was prepared according to the published procedure[1] using Airstone 760E/766H and 5 wt% of L-Cystine. The Recyclamine based composite material (Fig.4) is a product sample for wind turbine blades acquired from Aditya Birla Chemicals. Specification and source for Airstone 760E/766H, UHU 2-component glue, Roizefar Epoxy Resin, Sicomin SR infugreen 810/SD8822 and Litestone 3100E/3102H as well as the analysis on particle size can be found in a previously published article.[2]

2. Preparative Methods

2.1 Synthesis of Model Compounds

The synthesis of **Me-BPA**, **model 1**, 2-((4-(2-(4-methoxyphenyl)propan-2-yl)phenoxy)methyl)oxirane, **model 3** and **model 4** was carried according out to reported procedures.[2]

Ketone I (1,3-bis(4-(2-(4-methoxyphenyl)propan-2-yl)phenoxy)propan-2-one)

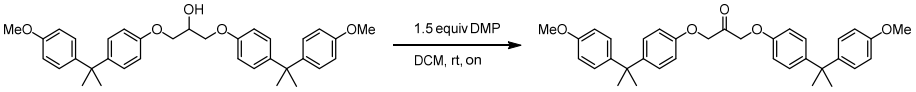

1.08 g (2.00 mmol, 1 equiv) of **model 1** was dissolved in 20 ml anhydrous DCM and 1.27 g (3.00 mmol, 1.5 equiv) of Dess-Martin Periodinane were added in portions. The reaction mixture was stirred at room temperature over-night. After the reaction was complete, as confirmed by TLC, the reaction mixture was diluted with H_2O and the organic phase extracted with three times using 20 ml of DCM. The organic phase was then washed with three times 20 ml of aq. $NaHCO_3$ and then dried over Na_2SO_4. The solvent was removed *in vacuo* and the residue was subject to flash column chromatography over silica using a gradient of pentane to 1/20 pentane/ethyl acetate affording the product in a yield of 60% (0.65 g, 1.21 mmol).

^{1}H NMR ($CDCl_3$, 400 MHz, 25 °C): δ = 7.17 – 7.11 (m, 8H), 6.82 – 6.79 (m, 8H), 4.85 (s, 4H), 3.78 (s, 6H), 1.64 (s, 12H) ppm; ^{13}C NMR ($CDCl_3$, 101 MHz, 25 °C): δ = 203.2 (s, 1C), 157.6 (s, 2C), 155.6 (s, 2C), 144.7 (s, 2C), 142.9 (s, 2C), 128.1 (d, 4C), 127.8 (d, 4C), 114.1 (d, 4C), 113.4 (d, 4C), 71.9 (t, 2C), 55.3 (q, 2C), 41.9 (s, 2C), 31.2 (q, 2C) ppm; HRMS (ESI+): calculated $[M+Na]^+$ = $[C_{35}H_{38}O_5+Na]^+$ 561.2611; found 561.2643.

Model 2 (1-(ethylamino)-3-(4-(2-(4-methoxyphenyl)propan-2-yl)phenoxy)propan-2-ol)

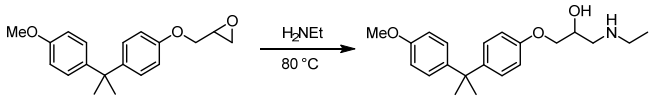

In a round bottom flask, 389 mg (1.30 mmol, 1 equiv) of 2-((4-(2-(4-methoxyphenyl)propan-2-yl)phenoxy)methyl)oxirane were mixed with 6.50 ml (5.20 g, 13.0 mmol, 10 equiv, 2M in THF) of ethylamine and stirred at 80 °C over-night, then cooled to room temperature. The residue was taken up in 25 ml of ethyl acetate and washed five times with 15 ml of brine, dried over $MgSO_4$ and filtered. The crude product was columned over silica gel using a gradient of 9/1 pentane/ethyl acetate to 45/25/30 pentane/ethyl acetate/methanol affording a yellow oil which precipitated in a freezer at -30 °C over-night. The product was then crystallized using methanol overlayered with diethyl ether and afforded a colourless solid over the course of a few days. The mother liquor was decanted off and the solid washed with pentane, affording the product in a yield of 82% (365 mg, 1.06 mmol).

R_f (ethyl acetate/methanol 1/1, silica gel) = 0.29; ^{1}H NMR ($CDCl_3$, 400 MHz, 25 °C): δ = 7.15 – 7.12 (m, 4H), 6.83 – 6.79 (m, 4H), 4.06 – 4.03 (m, 1H), 3.96 – 3.96 (m, 2H), 3.78 (s, 3H), 2.88 – 2.84 (m, 1H), 2.78 – 2.66 (m, 3H), 1.63 (s, 6H), 1.15 – 1.11 (m, 3H) ppm; ^{13}C NMR ($CDCl_3$, 101 MHz, 25 °C): δ = 157.5 (s, 1C), 156.6 (s, 1C), 143.7 (s, 1C), 143.2 (s, 1C), 127.9 (d, 2C), 127.8 (d, 2C), 114.0 (d, 2C), 113.4 (d, 2C), 70.6 (t, 1C), 68.4 (d, 1C), 55.3 (q, 1C), 51.8 (t, 1C), 44.2 (t, 1C), 41.8 (s, 1C), 31.2 (q, 2C), 15.5 (q, 1C) ppm; HRMS (ESI+): calculated $[M+H]^+$ = $[C_{26}H_{38}NO_3+H]^+$ 344.2220; found 344.2238.

1-(allyl(methyl)amino)-3-(4-(2-(4-methoxyphenyl)propan-2-yl)phenoxy)propan-2-ol

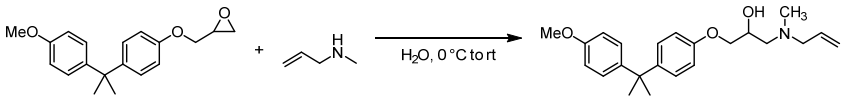

The synthesis was carried out according to the procedure reported for **model 3**.[2] The product was isolated using flash column chromatography over silica using a gradient of heptane to 1/5 EtOAc/MeOH in a yield of 36% (1.30 g, 0.36 mmol).

^{1}H NMR ($CDCl_3$, 400 MHz, 25 °C): δ = 7.16 – 7.12 (m, 4H), 6.84 – 6.78 (m, 4H), 5.85 (dddd, 1H, *J*=17.0, 10.1, 6.8, 6.2 Hz), 5.22 – 5.14 (m, 2H), 4.09 – 4.03 (m, 1H), 3.99 – 3.92 (m, 2H), 3.78 (s, 3H), 3.17 (ddt, 1H, *J*=13.7, 6.2, 1.4 Hz), 3.04 (ddt, 1H, *J*=13.6, 6.8, 1.2 Hz), 2.60 (dd, 1H, *J*=12.4, 9.7 Hz), 2.48 (dd,

1H, *J*=12.4, 3.9 Hz), 2.30 (s, 3H), 1.64 (s, 6H) ppm; ^{13}C NMR ($CDCl_3$, 101 MHz, 25 °C): δ = 157.5 (s, 1C), 156.7(s, 1C), 143.5 (s, 1C), 143.2 (s, 1C), 135.3 (d, 1C), 127.8 (d, 2C), 118.1 (t, 1C), 114.0 (d, 2C), 113.4 (d, 2C), 70.4 (t, 1C), 66.2 (d, 1C), 61.3 (t, 1C), 59.5 (t, 1C), 55.3 (q, 1C), 42.2 (q, 1C), 41.8 (s, 2C), 31.2(q, 2C) ppm; HRMS (ESI+): calculated $[M+Na]^+ = [C_{23}H_{32}NO_3]^+$ 370.2377; found 370.2361.

N-(2-methoxy-3-(4-(2-(4-methoxyphenyl)propan-2-yl)phenoxy)propyl)-N-methylprop-2-en-1-amine

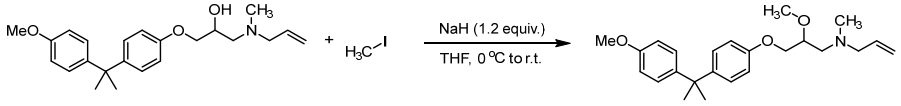

0.50 g (1.40 mmol, 1 equiv) of 1-(allyl(methyl)amino)-3-(4-(2-(4-methoxyphenyl)propan-2-yl)phenoxy)propan-2-ol was dissolved in 12 ml of dry THF under argon and cooled using a water/ice bath. 65.0 mg (1.60 mmol, 1.15 equiv, 60 wt% in mineral oil) of NaH was added in portions and then stirred for 1 h under cooling. 211 mg (1.50 mmol, 1.07 equiv) of MeI was added dropwise under cooling and the reaction mixture was stirred for 2 h. Then, the reaction mixture was quenched with methanol and the solvent was removed *in vacuo*. The residue was subject to automated flash column chromatography over silica using a gradient of heptane to 1/10 EtOAc/MeOH affording the product in a yield of 44% (229 mg, 0.60 mmol).

^{1}H NMR ($CDCl_3$, 400 MHz, 25 °C): δ = 7.16 – 7.11 (m, 4H), 6.84 – 6.78 (m, 4H), 5.84 (ddt, 1H, *J*=16.7, 10.1, 6.5 Hz), 5.19 – 5.10 (m, 2H), 4.07 (dd, 1H, *J*=10.0, 4.0 Hz), 3.97 (dd, 1H, *J*=10.0, 5.3 Hz), 3.78 (s, 3H), 3.69-3.64 (m, 1H), 3.49 (s, 3H), 3.05 (d, 2H, *J*=6.6 Hz), 2.56 (d, 2H, *J*=6.0 Hz), 2.29 (s, 3H), 1.60 (s, 6H) ppm; ^{13}C NMR ($CDCl_3$, 101 MHz, 25 °C): ^{13}C NMR ($CDCl_3$, 101 MHz): δ = 157.5 (s, 1C), 156.8 (s, 1C), 143.4 (s, 1C), 143.3 (s, 1C), 135.8 (d, 1C), 127.9 (d, 2C), 127.8 (d, 2C), 117.7 (t, 1C), 114.1(d, 2C), 113.4 (d, 2C), 78.2 (d, 1C), 68.8 (t, 1C), 61.8 (t, 1C), 58.0 (q, 1C), 57.9 (t, 1C), 55.3 (q, 1C), 43.3 (q, 1C), 41.8 (s, 1C), 31.2 (q, 2C) ppm; HRMS (ESI+): calculated $[M+Na]^+ = [C_{24}H_{34}NO_3]^+$ 384.2533; found 384.2502.

Model 5 (2-methoxy-3-(4-(2-(4-methoxyphenyl)propan-2-yl)phenoxy)-N-methylpropan-1-amine)

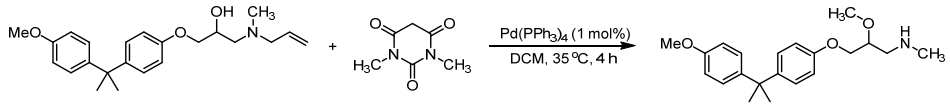

In an Argon-charged glovebox, 228 mg (0.60 mmol, 1 equiv) of 1-(allyl(methyl)amino)-3-(4-(2-(4-methoxyphenyl)propan-2-yl)phenoxy)propan-2-ol, 278 mg (1.78 mmol, 3 equiv) of 1,3-dimethylpyrimidine-2,4,6(1H,3H,5H)-trione and 6.90 mg (6.00 nm, 10 mol%) of $Pd(PPh_3)_4$ were dissolved in 15 ml of DCM and then heated to 35 °C for 4 h. After complete conversion, as confirmed by TLC, the solvent was removed *in vacuo*. The residue was taken up in 20 ml of diethyl which was then washed three times with saturated Na_2CO_3 solution. The organic phase was dried over Na_2SO_4 and the solvent was removed *in vacuo*. Automated flash column chromatography over silica using a gradient of heptane to MeOH afforded the product in a yield of 84% (171 mg, 0.50 mmol).

^{1}H NMR ($CDCl_3$, 400 MHz, 25 °C): δ = 7.15 – 7.11 (m, 4H), 6.83 – 6.78 (m, 4H), 4.01 (d, 2H, *J*=4.9 Hz), 3.78 (s, 3H), 3.74-3.69 (m, 1H), 3.50 (s, 3H), 2.84 – 2.76 (m, 2H), 2.47 (s, 3H), 2.41 (br, 1H), 1.63 (s, 6H) ppm; ^{13}C NMR ($CDCl_3$, 101 MHz, 25 °C): δ = 157.5 (s, 1C), 156.6 (s, 1C), 143.6 (s, 1C), 143.2 (s, 1C), 127.9 (d, 2C), 127.8 (d, 2C), 114.0 (d, 2C), 113.4 (d, 2C), 78.6 (d, 1C), 68.2 (t, 1C), 58.3 (q, 1C), 55.3 (q, 1C), 52.9 (t, 1C), 41.8 (s, 1C), 36.4 (q, 1C), 31.2 (q, 2C) ppm; HRMS (ESI+): calculated $[M+Na]^+ = [C_{21}H_{30}NO_3]^+$ 344.2220; found 344.2233.

2.2 Optimisations

For optimisation reactions using model compounds 54.0 mg (0.10 mmol, 1 equiv) of the substrate were dissolved in 2 ml of solvent in a 10 ml COtube, then appropriate reagents were added. After sealing the reaction vessel, the mixtures were stirred outside of the glovebox in aluminium heating blocks at 650 rpm. Sodium hydroxide was used as a powder. After the given reaction time, the reaction mixtures were quenched with 2 ml of 4 M hydrochloric acid and extracted using ethyl acetate. Yields are given for products isolated *via* flash column chromatography over silica.

Table S1. Optimisation of Tandem Dehydrogenation – Base-induced Cleavage Cascade on **Model 1**.

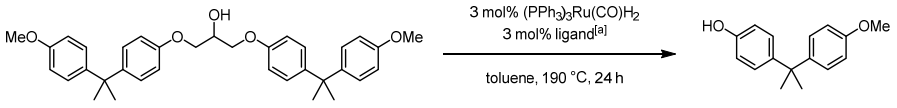

model 1 Me-BPA

Entry	Conditions / Variation	Consumption	Me-BPA
1	none	4%	0%
2	10 mol% NaO*t*Bu	56%	17%
2	3 equiv NaO*t*Bu	100%	76%
3	3 equiv NaO*t*Bu, 170 °C	80%	51%
4	3 equiv NaO*t*Bu, 150 °C	32%	26%
5	6 equiv NaO*t*Bu	100%	73%
6	6 equiv NaOH	100%	68%
7	6 equiv NaOH, no [Ru], no ligand	60%	34%

[a] Bis[(2-diphenylphosphino)ethyl]ammonium chloride.

For optimisation reactions on polymeric sample powdered Airstone 760E/766H (BPA content of approx. 43 wt%) was chosen as a benchmark system. 100 mg (approx. 0.188 mmol BPA, 1 equiv) of powdered resin were suspended in 4.2 ml of solvent in a 40 ml COtube, then appropriate reagents were added. Sodium hydroxide was used as a powder. After sealing the reaction vessel, the mixtures were stirred outside of the glovebox in aluminium heating blocks at 300 rpm. After the given reaction time, the reaction mixtures were quenched with 10 ml of 4 M hydrochloric acid and extracted using ethyl acetate. Yields are given for product isolated *via* flash column chromatography over silica. The corresponding tables can be found in the manuscript (Fig. 2c, Table 1, Table 2).

2.3 Deconstruction of Model Compounds

General Procedure for Deconstructing Model Compounds

54.0 mg (0.10 mmol, 1 equiv) of the substrate were dissolved in 2 ml of toluene in a 10 ml COtube under air, then 24.0 mg (0.60 mmol, 6 equiv) of powdered sodium hydroxide were added. After sealing the reaction vessel, the mixtures were stirred outside of the glovebox in aluminium heating blocks at 650 rpm at 190 °C. After the given reaction time, the reaction mixtures were quenched with 2 ml of 4 M hydrochloric acid and extracted using ethyl acetate. Yields are given for product isolated *via* flash column chromatography over silica using 10/1 pentane/ethyl acetate as eluent. For substrates that can liberate two Me-BPA, full conversion is considered corresponding to cleavage of both possible bonds.

Deconstruction of Model 1

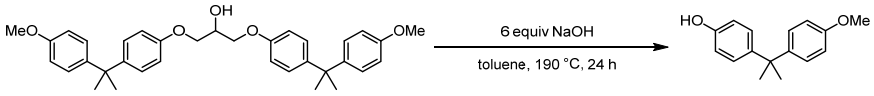

model 1 **Me-BPA**

The reaction was carried out according to the general procedure. 54.0 mg (0.10 mmol, 1 equiv) of model 1, 24.0 mg (0.60 µmol, 6 equiv) of powdered sodium hydroxide and 2 mol of toluene were used. Me-BPA was isolated as colourless oil in a yield of 34% (16.4 mg, 70.0 nmol).

R_f (pentane/ethyl acetate 4/1, silica gel) = 0.3; ^{1}H NMR ($CDCl_3$, 400 MHz, 25 °C): δ = 7.16 – 7.14 (m, 2H), 7.11 – 7.09 (m, 2H), 6.83 – 6.81 (m, 2H), 6.74 – 6.72 (m, 2H), 4.76 (s, 1H), 3.80 (s, 3H), 1.64 (s, 6H) ppm. The NMR spectra are in agreement with reported data[3].

Deconstruction of Ketone 1

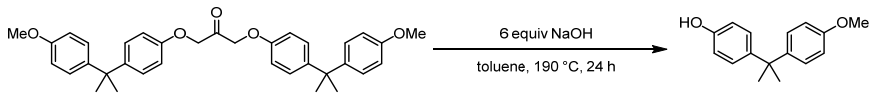

ketone 1 **Me-BPA**

The reaction was carried out according to the general procedure. 53.9 mg (0.10 mmol, 1 equiv) of ketone 1, 24.0 mg (0.60 µmol, 6 equiv) of powdered sodium hydroxide and 2 mol of toluene were used. Me-BPA was isolated as colourless oil in a yield of 82% (39.8 mg, 164 nmol).

R_f (pentane/ethyl acetate 4/1, silica gel) = 0.3; ^{1}H NMR ($CDCl_3$, 400 MHz, 25 °C): δ = 7.16 – 7.14 (m, 2H), 7.11 – 7.09 (m, 2H), 6.83 – 6.81 (m, 2H), 6.74 – 6.72 (m, 2H), 4.76 (s, 1H), 3.80 (s, 3H), 1.64 (s, 6H) ppm. The NMR spectra are in agreement with reported data[3].

Deconstruction of Model 2

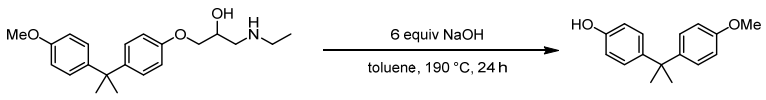

model 2 **Me-BPA**

The reaction was carried out according to the general procedure. 34.3 mg (0.10 mmol, 1 equiv) of model 2, 24.0 mg (0.60 µmol, 6 equiv) of powdered sodium hydroxide and 2 mol of toluene were used. Me-BPA was isolated as colourless oil in a yield of 68% (16.4 mg, 67.5 nmol).

R_f (pentane/ethyl acetate 4/1, silica gel) = 0.3; ^{1}H NMR ($CDCl_3$, 400 MHz, 25 °C): δ = 7.16 – 7.14 (m, 2H), 7.11 – 7.09 (m, 2H), 6.83 – 6.81 (m, 2H), 6.74 – 6.72 (m, 2H), 4.76 (s, 1H), 3.80 (s, 3H), 1.64 (s, 6H) ppm. The NMR spectra are in agreement with reported data[3].

Deconstruction of Model 3

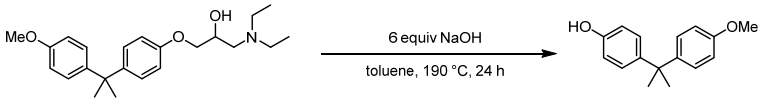

model 3 **Me-BPA**

The reaction was carried out according to the general procedure. 37.2 mg (0.10 mmol, 1 equiv) of model 3, 24.0 mg (0.60 µmol, 6 equiv) of powdered sodium hydroxide and 2 mol of toluene were used. Me-BPA was isolated as colourless oil in a yield of 61% (14.8 mg, 61.1 nmol).

R_f (pentane/ethyl acetate 4/1, silica gel) = 0.3; ^{1}H NMR ($CDCl_3$, 400 MHz, 25 °C): δ = 7.16 – 7.14 (m, 2H), 7.11 – 7.09 (m, 2H), 6.83 – 6.81 (m, 2H), 6.74 – 6.72 (m, 2H), 4.76 (s, 1H), 3.80 (s, 3H), 1.64 (s, 6H) ppm. The NMR spectra are in agreement with reported data[3].

Deconstruction of Model 4

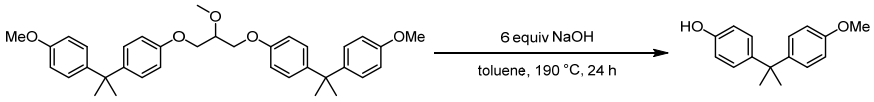

model 4 **Me-BPA**

The reaction was carried out according to the general procedure. 55.4 mg (0.10 mmol, 1 equiv) of model 4, 24.0 mg (0.60 µmol, 6 equiv) of powdered sodium hydroxide and 2 mol of toluene were used. No consumption was observed.

Deconstruction of Model 5

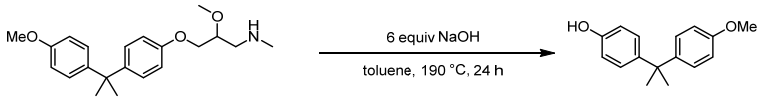

model 5 **Me-BPA**

The reaction was carried out according to the general procedure. 34.3 mg (0.10 mmol, 1 equiv) of model 5, 24.0 mg (0.60 µmol, 6 equiv) of powdered sodium hydroxide and 2 mol of toluene were used. No consumption was observed.

2.4 Deconstruction of Resins

General Procedure for Deconstructing Epoxy Resins

100 mg of powdered resin were suspended in 4.2 ml of solvent in a 40 ml COtube under air, then 50 wt% of powdered sodium hydroxide was added. After sealing the reaction vessel, the mixtures were stirred outside of the glovebox in aluminium heating blocks at 300 rpm at 190 °C. After the given reaction time, the reaction mixtures were quenched with 10 ml of 4 M hydrochloric acid and extracted using ethyl acetate. The remaining reaction mixture is transferred into a round bottom flask. Celite® is added and the solvent removed *in vacuo*. The resulting powder is loaded onto a silica gel charged column. Column chromatography using gradient of 6/1 pentane/ethyl acetate to 4/1 pentane/ethyl acetate affords bisphenol A.

The deconstruction of **Airstone 760E/766H** (approx. BPA content 43 wt%) was carried out according to the general procedure. 100 mg (approx. 0.188 mmol BPA, 1 equiv) of powdered resin, 50 mg (1.25 mmol, 6.6 equiv) of powdered sodium hydroxide and 4.2 ml of toluene were used. Column chromatography afforded BPA as a colourless solid.

BPA: Yield of 81% (34.7 mg, 152 µmol); R_f (pentane/ethyl acetate 4/1, silica gel) = 0.21; ^{1}H NMR ($CDCl_3$, 400 MHz, 25 °C): δ = 7.11 – 7.07 (m, 4H), 6.76 – 6.70 (m, 4H), 4.57 (s, 2H), 1.62 (s, 6H) ppm. The NMR spectra are in agreement with reported data.[4]

The deconstruction of **UHU 2-component glue** (approx. BPA content 34 wt%) was carried out according to the general procedure. 100 mg (approx. 0.148 mmol BPA, 1 equiv) of powdered resin, 50 mg (1.25 mmol, 8.5 equiv) of powdered sodium hydroxide and 4.2 ml of toluene were used. Column chromatography afforded BPA as a colourless solid.

BPA: Yield of 84% (28.5 mg, 125 µmol); R_f (pentane/ethyl acetate 4/1, silica gel) = 0.21; ^{1}H NMR ($CDCl_3$, 400 MHz, 25 °C): δ = 7.11 – 7.07 (m, 4H), 6.76 – 6.70 (m, 4H), 4.57 (s, 2H), 1.62 (s, 6H) ppm. The NMR spectra are in agreement with reported data.[4]

The deconstruction of **Roizefar Epoxy Resin** (approx. BPA content 30 wt%) was carried out according to the general procedure. 100 mg (approx. 0.131 mmol BPA, 1 equiv) of powdered resin, 50 mg (1.25 mmol, 9.5 equiv) of powdered sodium hydroxide and 4.2 ml of toluene were used. Column chromatography afforded BPA as a colourless solid.

BPA: Yield of 86% (25.9 mg, 113 µmol); R_f (pentane/ethyl acetate 4/1, silica gel) = 0.21; ^{1}H NMR ($CDCl_3$, 400 MHz, 25 °C): δ = 7.11 – 7.07 (m, 4H), 6.76 – 6.70 (m, 4H), 4.57 (s, 2H), 1.62 (s, 6H) ppm. The NMR spectra are in agreement with reported data.[4]

The deconstruction of **Sicomin SR infugreen 810/SD8822** (approx. BPA content 36 wt%) was carried out according to the general procedure. 100 mg (approx. 0.158 mmol BPA, 1 equiv) of powdered resin, 50 mg (1.25 mmol, 7.9 equiv) of powdered sodium hydroxide and 4.2 ml of toluene were used. Column chromatography afforded BPA as a colourless solid.

BPA: Yield of 56% (21.0 mg, 92.0 µmol); R_f (pentane/ethyl acetate 4/1, silica gel) = 0.21; ^{1}H NMR ($CDCl_3$, 400 MHz, 25 °C): δ = 7.11 – 7.07 (m, 4H), 6.76 – 6.70 (m, 4H), 4.57 (s, 2H), 1.62 (s, 6H) ppm. The NMR spectra are in agreement with reported data.[4]

The deconstruction of **Litestone 3100E/3102H** (approx. BPA content 33 wt%) was carried out according to the general procedure. 100 mg (approx. 0.145 mmol BPA, 1 equiv) of powdered resin, 50 mg (1.25 mmol, 8.6 equiv) of powdered sodium hydroxide and 4.2 ml of toluene were used. Column chromatography afforded BPA as a colourless solid.

BPA: Yield of 57% (18.8 mg, 82.3 µmol); R_f (pentane/ethyl acetate 4/1, silica gel) = 0.21; ^{1}H NMR ($CDCl_3$, 400 MHz, 25 °C): δ = 7.11 – 7.07 (m, 4H), 6.76 – 6.70 (m, 4H), 4.57 (s, 2H), 1.62 (s, 6H) ppm. The NMR spectra are in agreement with reported data.[4]

The deconstruction of **acid-disassembled L-Cystine-based resin** (BPA content unknown) was carried out according to the general procedure. 100 mg of powdered resin, 50 mg of powdered sodium hydroxide and 4.2 ml of toluene were used. Column chromatography afforded BPA as a colourless solid.

BPA: Yield of 22 wt% (22.3 mg, 97.7 µmol); R_f (pentane/ethyl acetate 4/1, silica gel) = 0.21; ^{1}H NMR ($CDCl_3$, 400 MHz, 25 °C): δ = 7.11 – 7.07 (m, 4H), 6.76 – 6.70 (m, 4H), 4.57 (s, 2H), 1.62 (s, 6H) ppm. The NMR spectra are in agreement with reported data.[4]

The deconstruction of **acid-disassembled Recyclamine-based resin** (BPA content unknown) was carried out according to the general procedure. 100 mg of powdered resin, 50 mg of powdered sodium hydroxide and 4.2 ml of toluene were used. Column chromatography afforded BPA as a colourless solid.

BPA: Yield of 15 wt% (15.1 mg, 66.1 µmol); R_f (pentane/ethyl acetate 4/1, silica gel) = 0.21; ^{1}H NMR ($CDCl_3$, 400 MHz, 25 °C): δ = 7.11 – 7.07 (m, 4H), 6.76 – 6.70 (m, 4H), 4.57 (s, 2H), 1.62 (s, 6H) ppm. The NMR spectra are in agreement with reported data.[4]

2.4 Aquatic work up only

500 mg of powdered Airstone 760E/766H and 250 mg (6.25 mmol, 50 wt%) of powdered sodium hydroxide were suspended in 15 ml of toluene in a 40 ml COtube under air. After sealing the reaction vessel, the mixtures were stirred outside of the glovebox in aluminium heating blocks at 300 rpm at 190 °C. After the given reaction time, the reaction mixtures were quenched with 8 ml of 4 M hydrochloric acid and extracted four times using 6 ml of ethyl acetate each. The united organic phase was dried of $MgSO_4$ and filtered over Celite. The solvent was removed in vacuo, affording 221 mg of crude BPA as an off white solid in a purity of 91.3% according to GC-MS analysis (Olin Corporation).

^{1}H NMR spectrum of BPA recovered via aquatic work up (in $(CD_3)_2CO$):

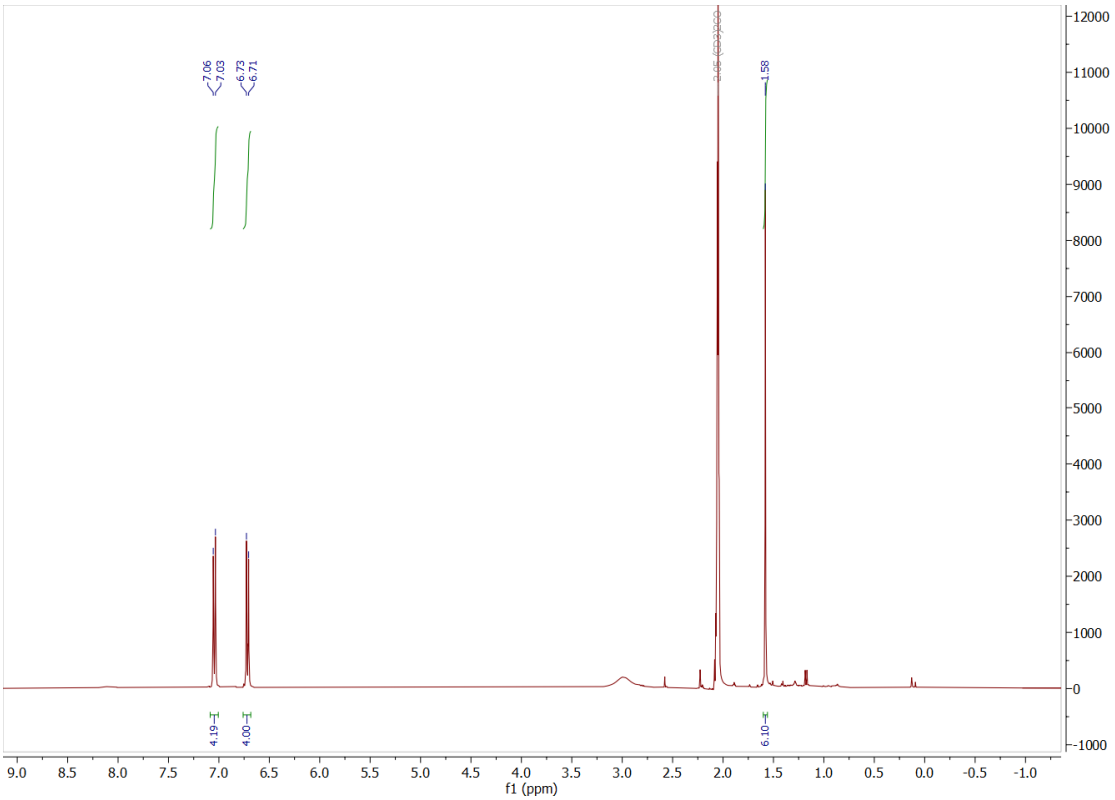

GC-MS Analysis of BPA recovered via aquatic work up:

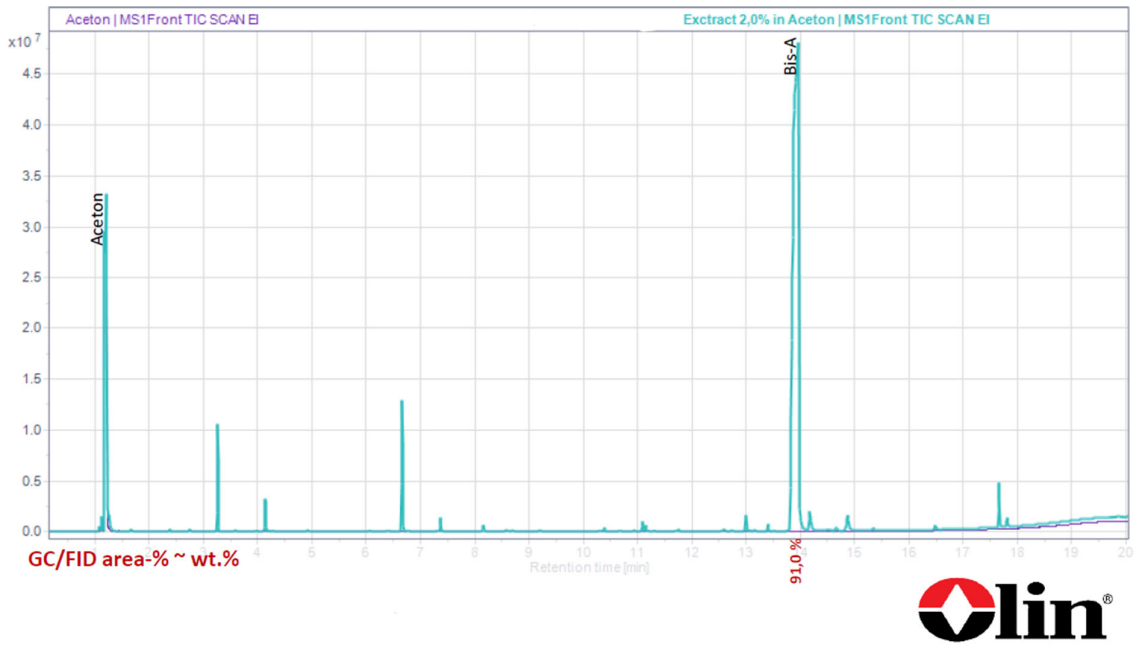

2.5 Deconstruction on 1 g scale

General Procedure for 1 g of Resin

A 30 mL PTFE inlay for high pressure reactor was charged with 1 g of powdered resin, 50 wt% (0.5 g) of powdered sodium hydroxide and 12 ml of toluene under air. After sealing the reactor the suspension was stirred at 190 °C at 300 rpm for 24 h. After cooling to rt, the reaction mixture was quenched with 10 ml of 4 M hydrochloric acid and extracted with three times 20 ml of ethyl acetate. The organic phase is transferred into a round bottom flask. Celite® is added and the solvent removed *in vacuo*. The resulting powder is loaded onto a silica gel charged column. Column chromatography using gradient of 6/1 pentane/ethylacetate to 4/1 pentane/ethyl acetate affords bisphenol A.

The deconstruction of **acid-disassembled L-Cystine-based resin** (BPA content unknown) was carried out according to the general procedure. 1.00 g of powdered resin, 0.50 g of powdered sodium hydroxide and 12 ml of toluene were used. Column chromatography afforded BPA as a colourless solid.

BPA: Yield of 28 wt% (283 mg, 1.24 mmol); R_f (pentane/ethyl acetate 4/1, silica gel) = 0.21; ^{1}H NMR ($CDCl_3$, 400 MHz, 25 °C): δ = 7.11 – 7.07 (m, 4H), 6.76 – 6.70 (m, 4H), 4.57 (s, 2H), 1.62 (s, 6H) ppm. The NMR spectra are in agreement with reported data.[4]

The deconstruction of **acid-disassembled Recyclamine-based resin** (BPA content unknown) was carried out according to the general procedure. 100 mg of powdered resin, 50 mg of powdered sodium hydroxide and 4.2 ml of toluene were used. Column chromatography afforded BPA as a colourless solid.

BPA: Yield of 7 wt% (70.2 mg, 0.31 mmol); R_f (pentane/ethyl acetate 4/1, silica gel) = 0.21; ^{1}H NMR ($CDCl_3$, 400 MHz, 25 °C): δ = 7.11 – 7.07 (m, 4H), 6.76 – 6.70 (m, 4H), 4.57 (s, 2H), 1.62 (s, 6H) ppm. The NMR spectra are in agreement with reported data.[4]

3. NMR Spectra

Ketone 1 (1,3-bis(4-(2-(4-methoxyphenyl)propan-2-yl)phenoxy)propan-2-one)

a) ^{1}H NMR spectrum

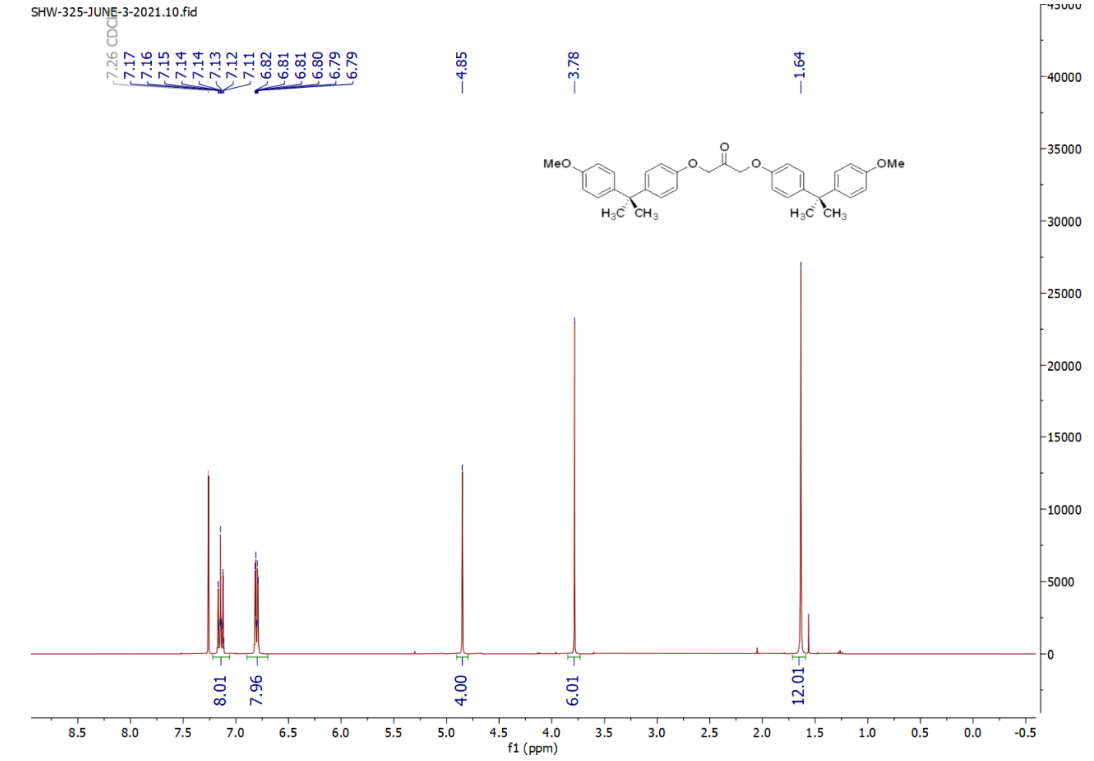

b) ^{13}C NMR spectrum

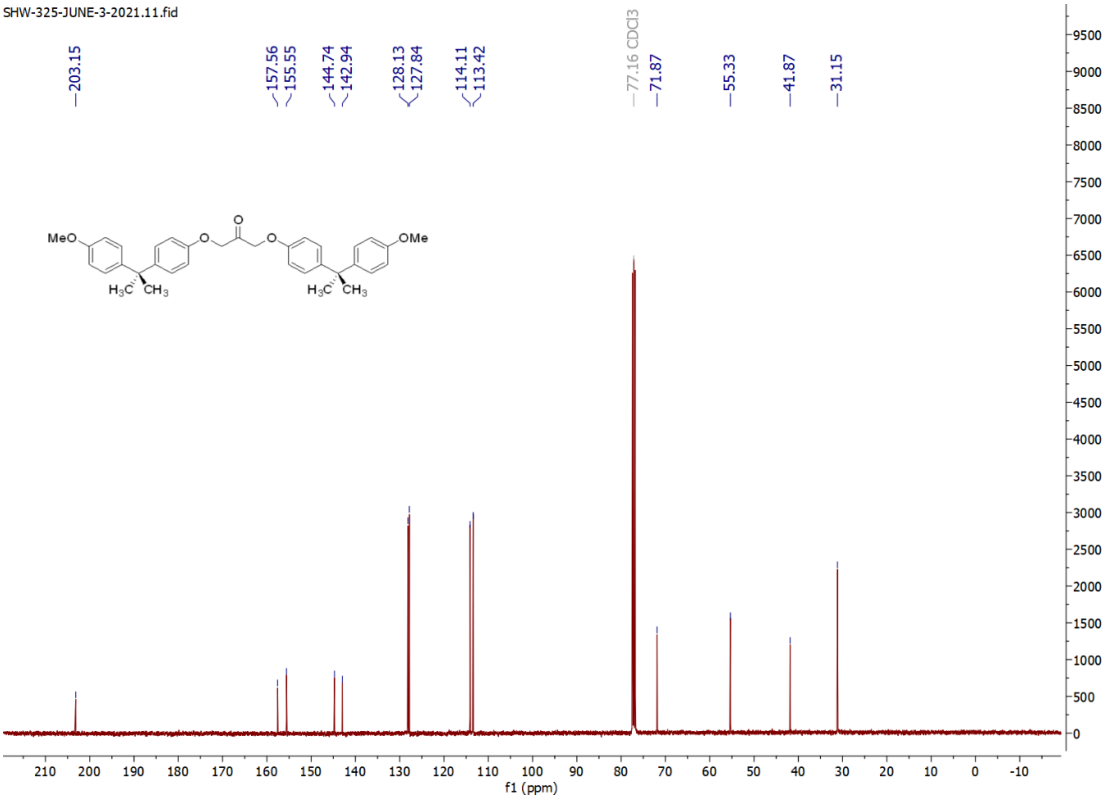

Model 2 (1-((ethyl)amino)-3-(4-(2-(4-methoxyphenyl)propan-2-yl)phenoxy)propan-2-ol)

a) ^{1}H NMR spectrum

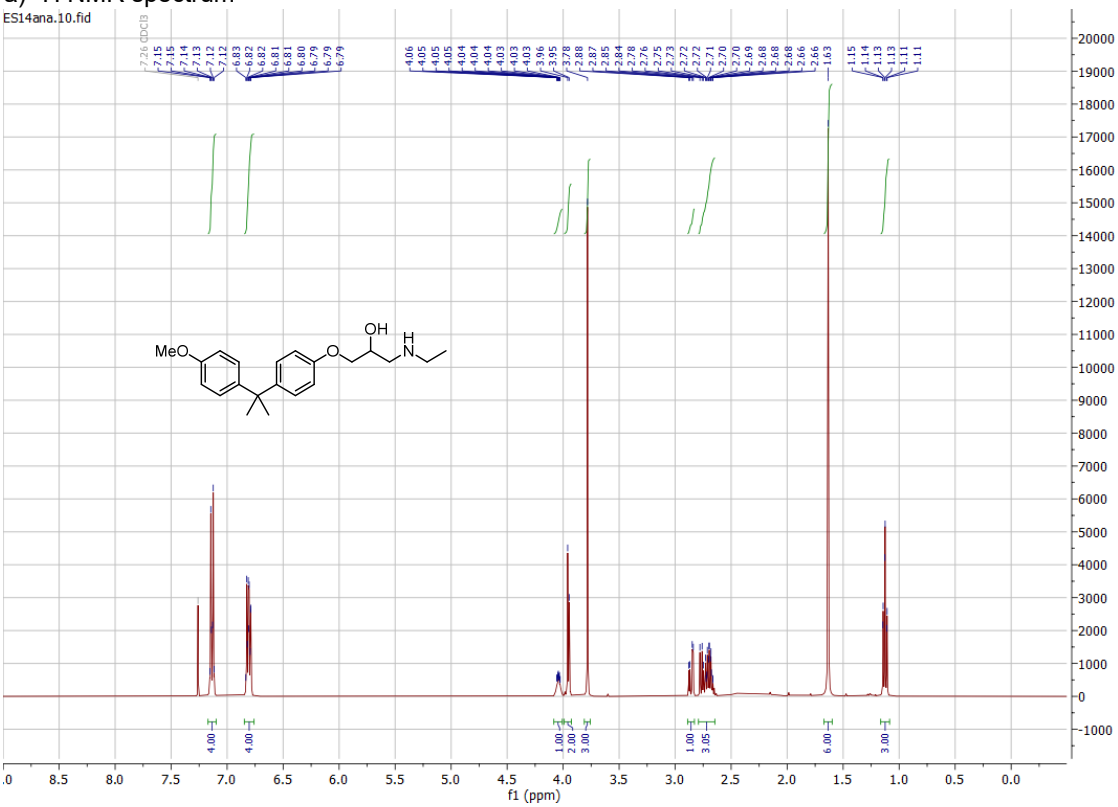

b) ^{13}C NMR spectrum

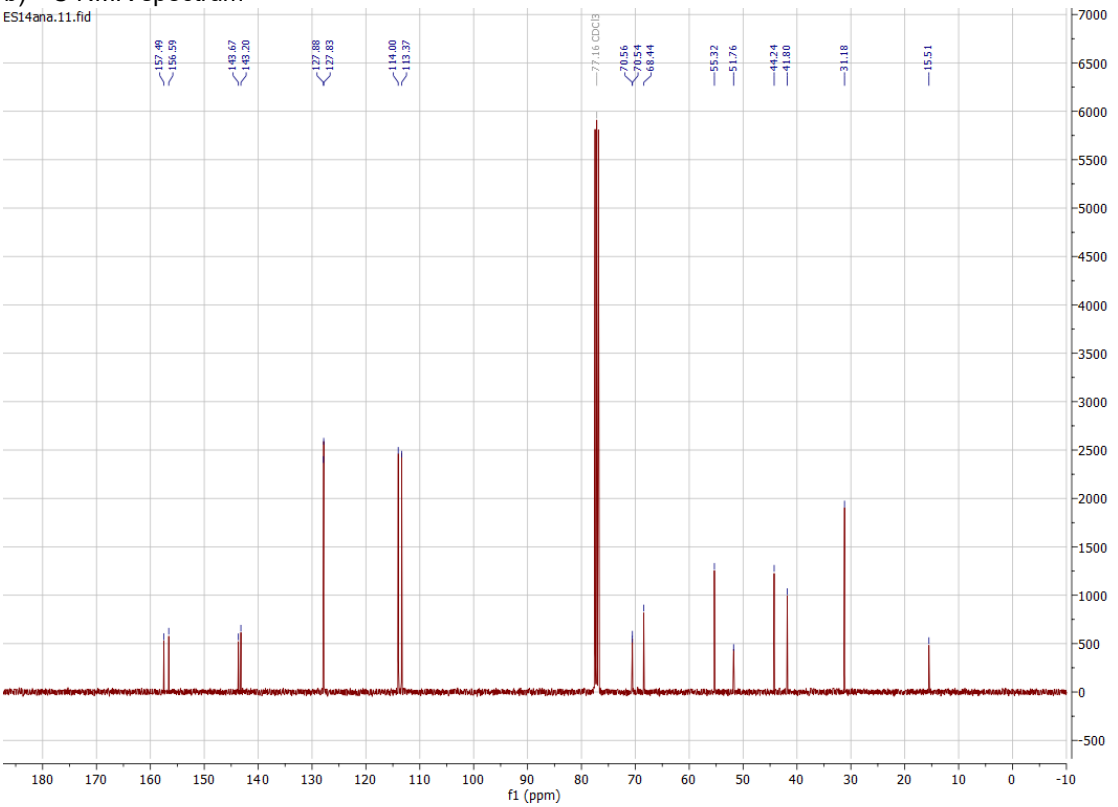

1-(allyl(methyl)amino)-3-(4-(2-(4-methoxyphenyl)propan-2-yl)phenoxy)propan-2-ol

a) ^{1}H NMR spectrum

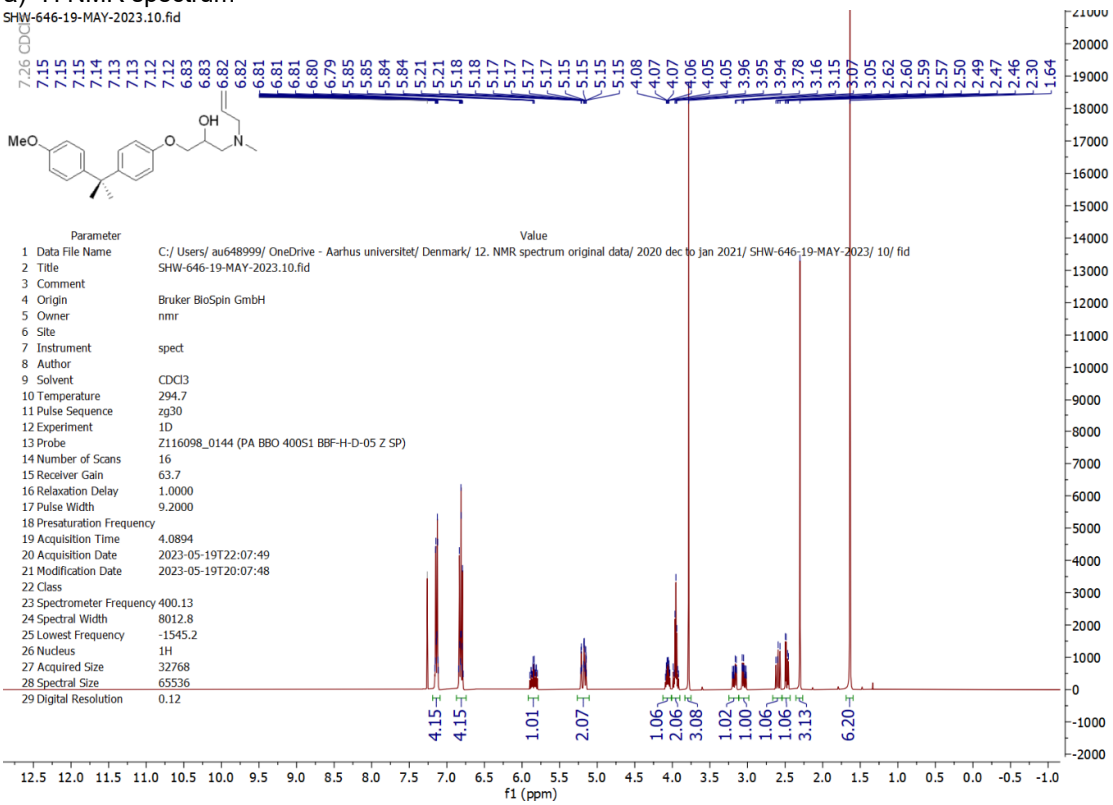

b) ^{13}C NMR spectrum

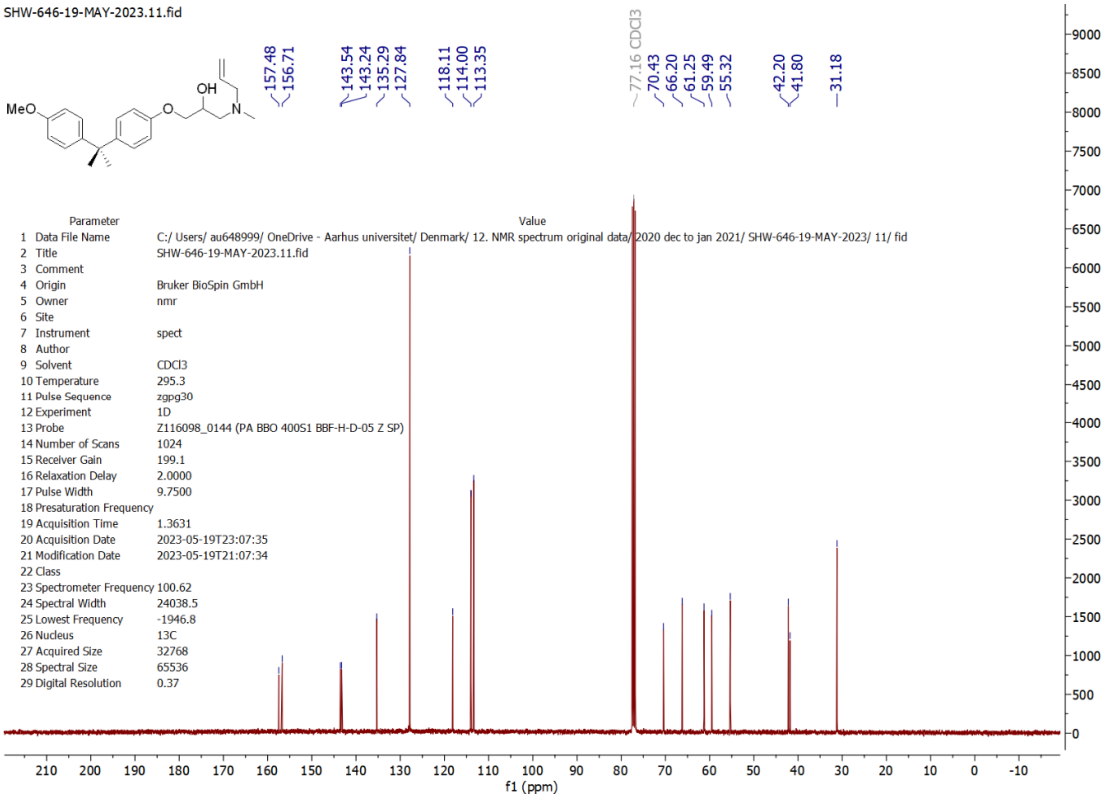

N-(2-methoxy-3-(4-(2-(4-methoxyphenyl)propan-2-yl)phenoxy)propyl)-N-methylprop-2-en-1-amine

a) ^{1}H NMR spectrum

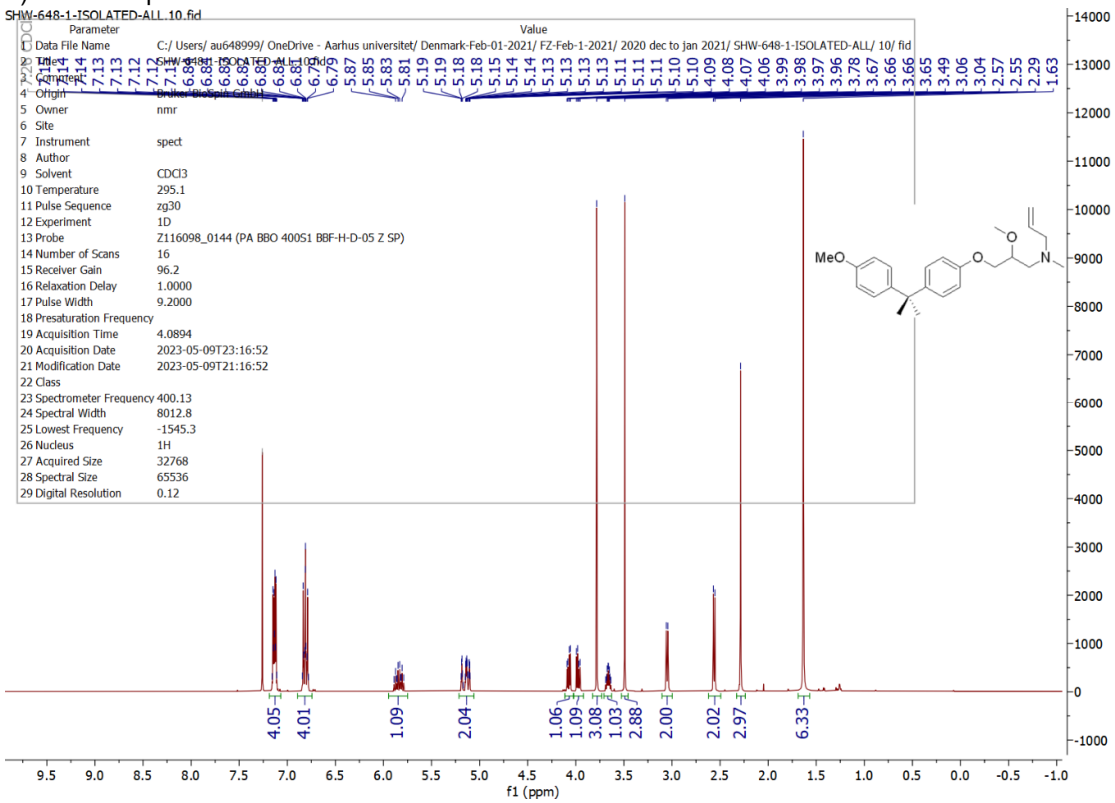

b) ^{13}C NMR spectrum

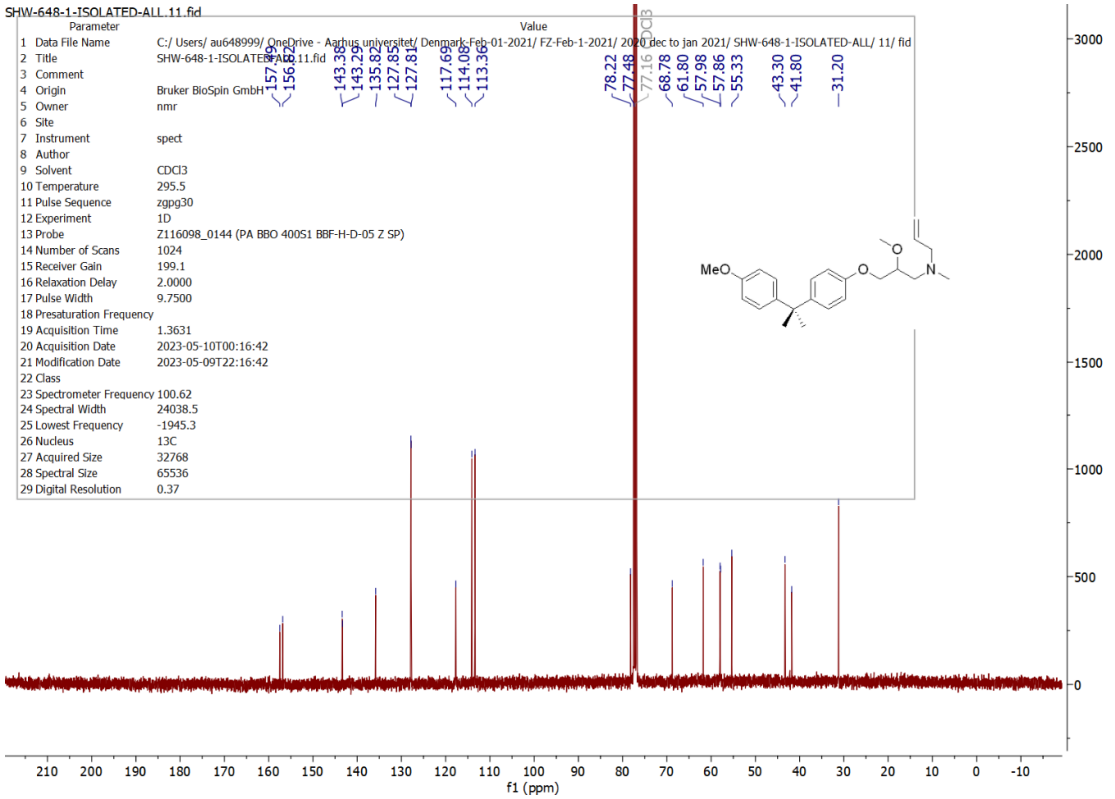

Model 5 (2-methoxy-3-(4-(2-(4-methoxyphenyl)propan-2-yl)phenoxy)-N-methylpropan-1-amine)

a) ^{1}H NMR spectrum

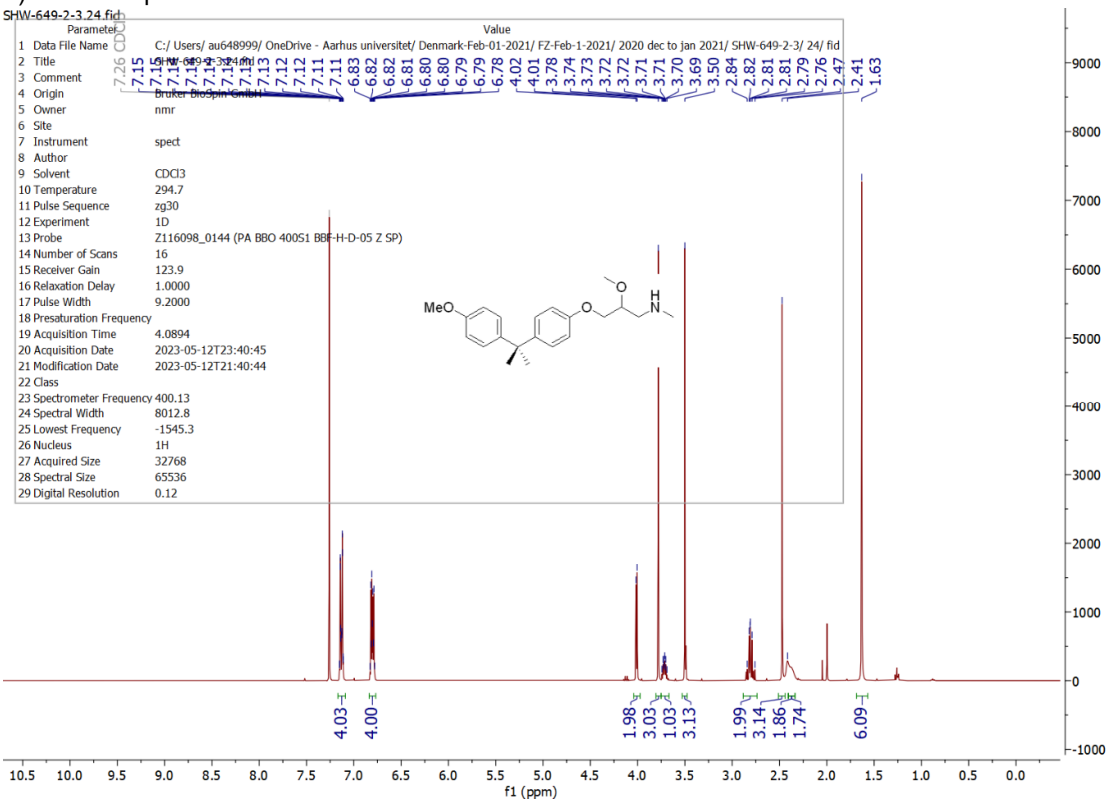

b) ^{13}C NMR spectrum

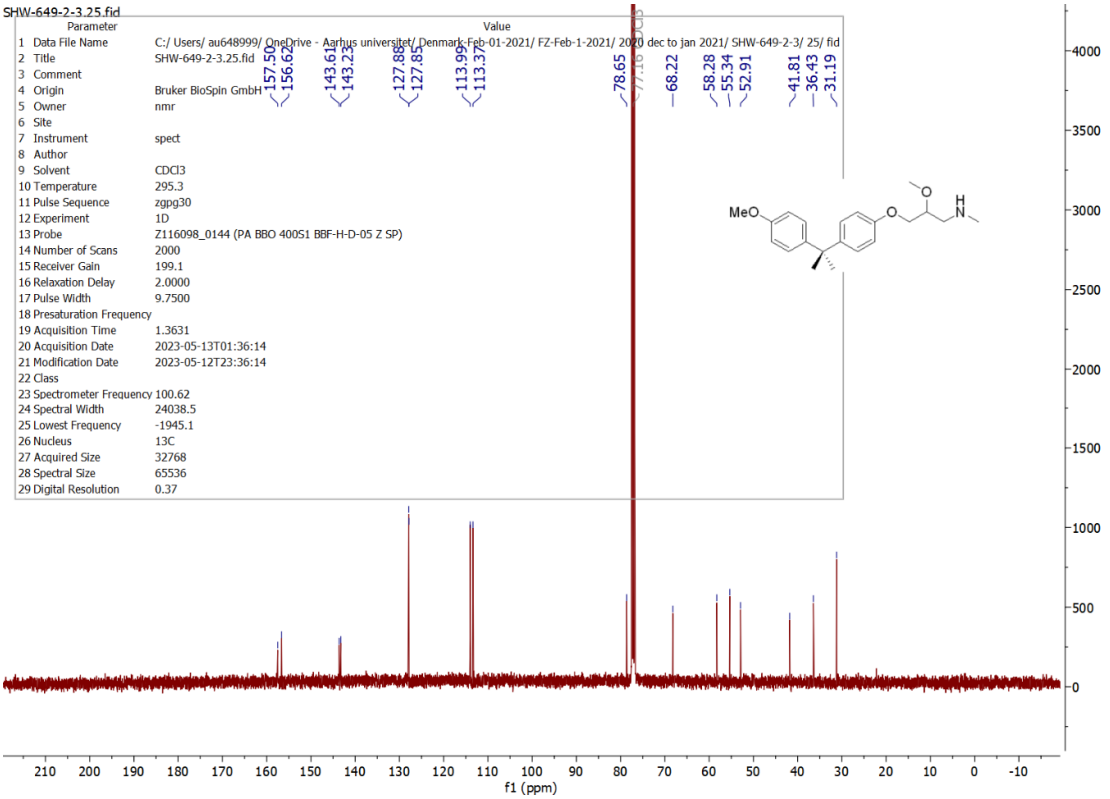

4. Density Function Theory

4.1 Alternative Mechanism Investigated

An SN2-like mechanism for the C-O bond cleavage at high temperatures with hydroxide anion was also considered for Models A-D. For Model A a barrier of only 21.1 kcal mol^{-1} is observed while for models B, C and D higher barriers were obtained.

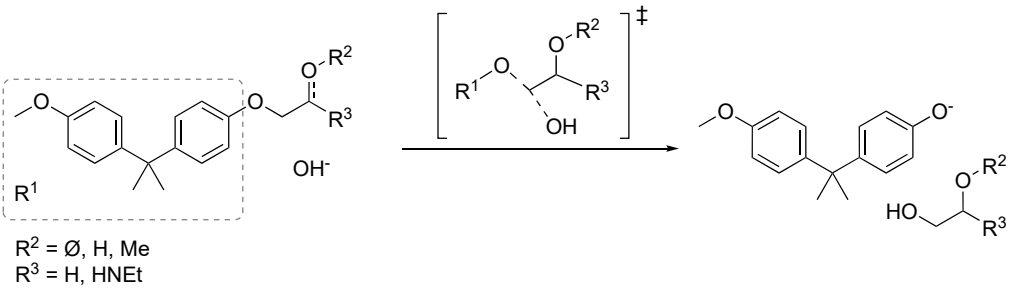

R^2 = Ø, H, Me
R^3 = H, HNEt

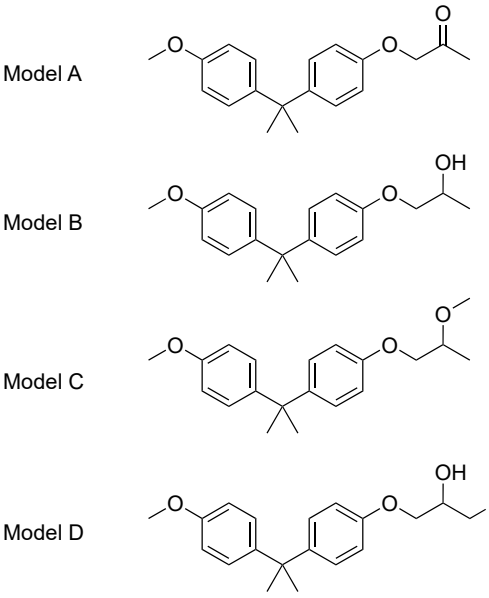

Model	$\Delta G^{‡}$ (Kcal mol^{-1})
A	21.1
B	37.1
C	35.9
D	40.1

Figure S3. Nucleophilic substitution pathway computed for Models A – D with free energies in kcal mol^{-1}.

Although Model A has a feasible barrier for the SN2-like mechanism we decided to further investigate if deprotonation of the alpha proton followed by an attack to a form cyclopropyl intermediate **A4** is viable. Although the deprotonation step occurs with a low barrier, the C–O bond cleavage step is highly energetic demanding thus making the SN2-like mechanism more feasible for Model A.

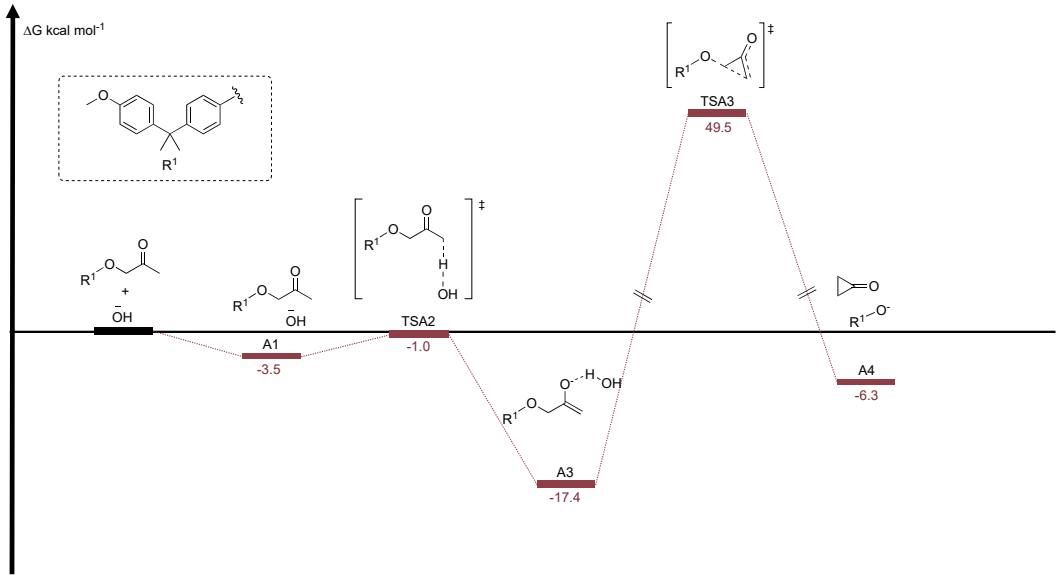

Figure S4: Second reaction pathway computed for Model A with free energies in kcal mol^{-1}.

For Model B and D deprotonation of the alcohol followed by an epoxide closure would lead to the C–O bond cleavage. The calculated mechanism starts with the H-bond interaction of hydroxide with Model B leading to **B1**, barrierless deprotonation leads to **B2** in which water is still interacting with the alkoxide anion. **B2** is in equilibrium with **B3** which has the free anion. The C–O bond cleavage step can undergo via **TSB2** or **TSB3**, for Model B **TSB2** is favored and an overall barrier of 26.3 kcal mol^{-1} was calculated. After this step, the epoxide **B4** is formed and its opening with hydroxide is thermodynamically favored to form **B5**.

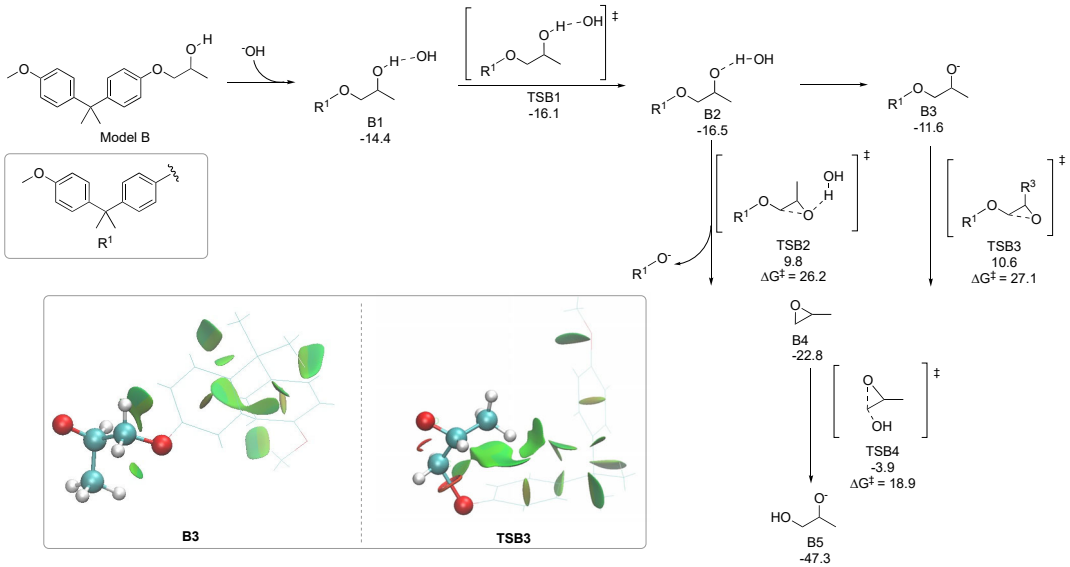

Figure S5. Reaction pathways proposed for Model B with free energies in kcal mol^{-1}.

The stabilisation of **D3** and **TSD3** with Model D, thanks to the hydrogen bond with the amine motif, favors **TSD3** over **TSD2**. The hydrogen bond interaction could be observed with an NCI-plot analysis. In a similar manner as for Model B, the opening of **D4** with hydroxide is thermodynamically favored leading to **D5**. The overall energy barrier for the reaction is 25.0 kcal mol^{-1}.

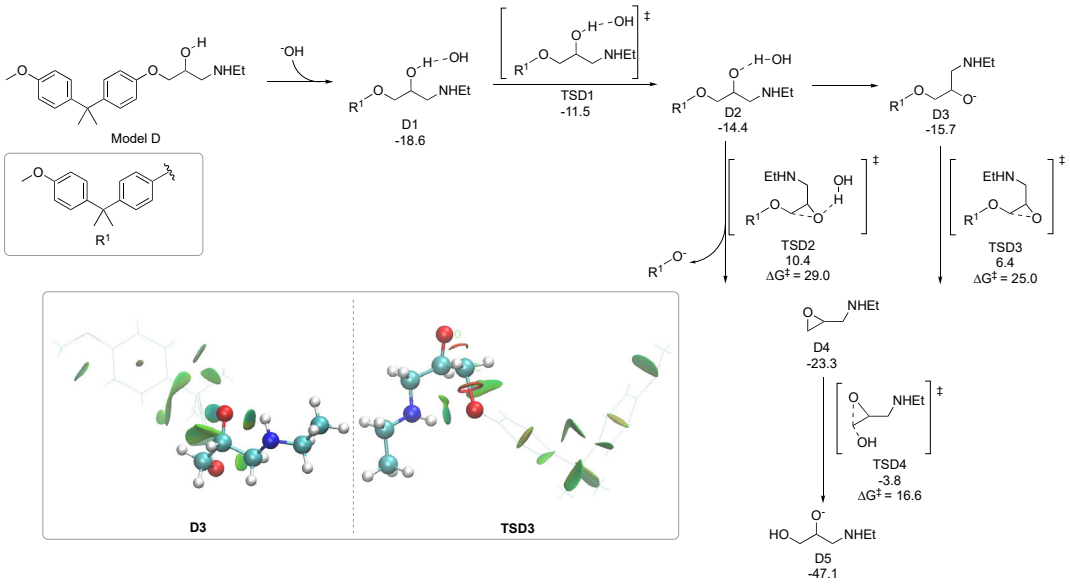

Figure S6. Reaction pathways proposed for Model D with free energies in kcal mol^{-1}.

The step of opening epoxide intermediate **B4** with hydroxide or R^1O^- was also studied. The opening in the terminal position with hydroxide is favored both kinetically and thermodynamically.

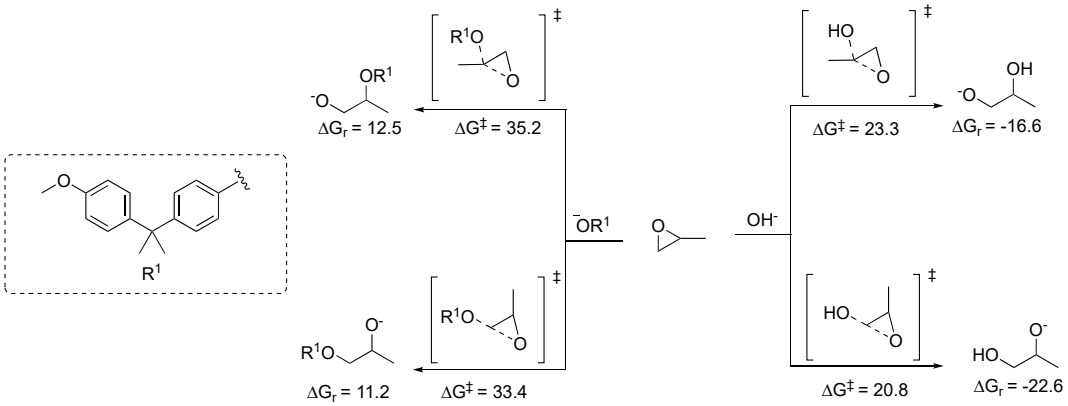

Figure S7. Reaction pathways computed for the opening of B4 with free energies in kcal mol^{-1}.

With Model D, the deprotonation of the alcohol by the amine motif in a concerted manner was also investigated. This mechanism has a high barrier of 63.5 kcal mol^{-1}.

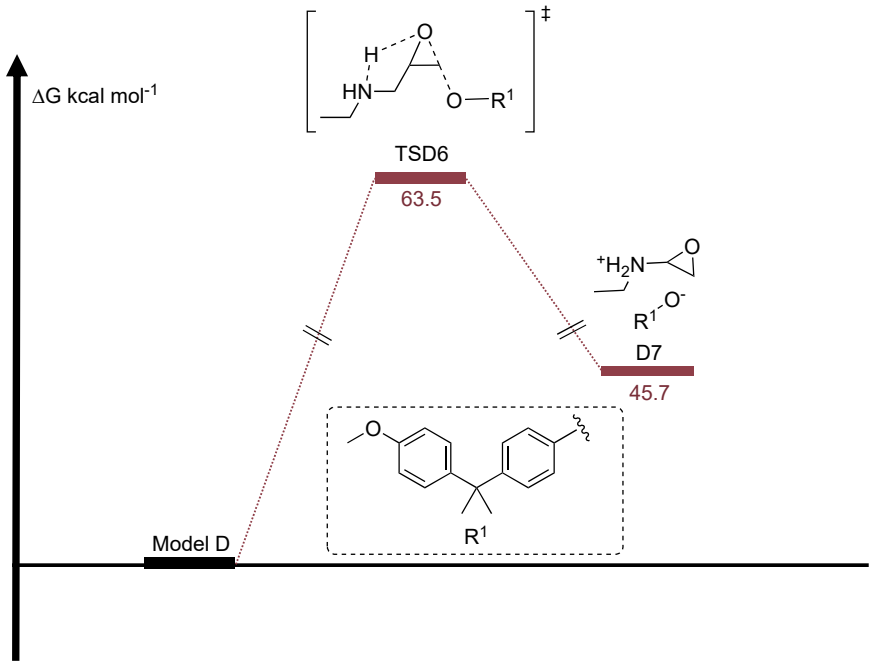

Figure S8. Third reaction pathway computed for Model D with free energies in kcal mol^{-1}.

Non-covalent interaction figures:

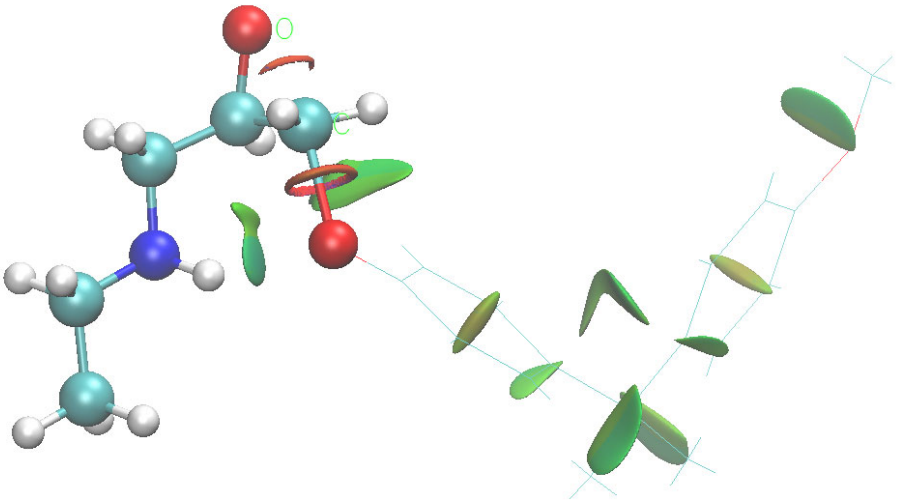

Figure S9. Non-covalent interaction plot of TSD3.

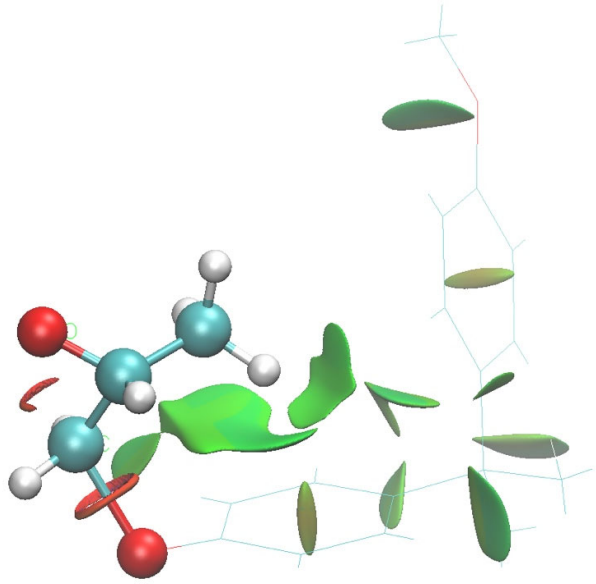

Figure S10. Non-covalent interaction plot of TSB3.

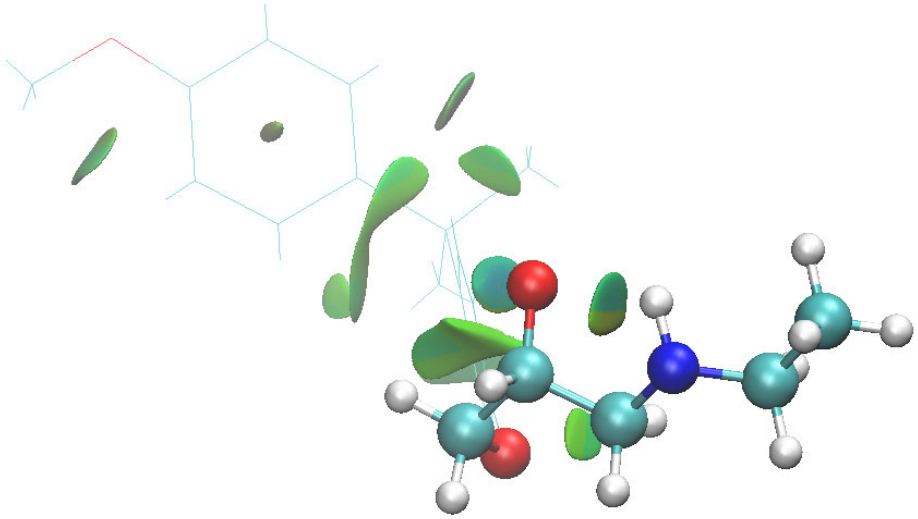

Figure S11. Non-covalent interaction plot of D3.

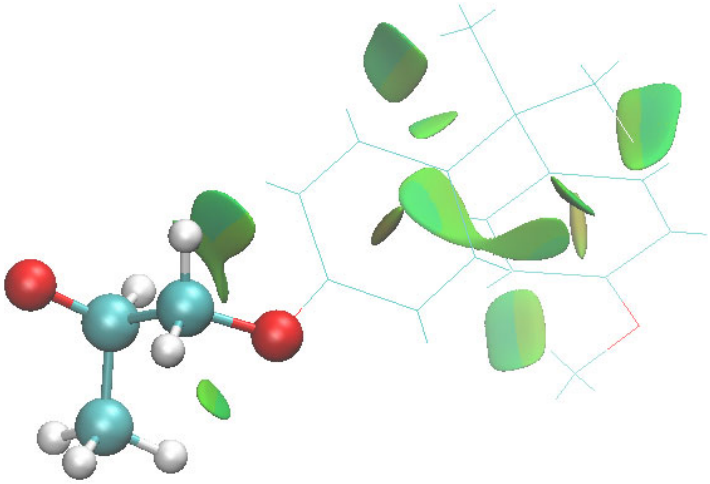

Figure S12. Non-covalent interaction plot of B3.

4.2 Computational details:

All density functional theory (DFT) results presented in this paper were performed in the Gaussian 16 package, at 463.15 K and 1 atm pressure.[5] The geometry optimization of all molecules was executed at the M06-2X/6-311++G(d,p) level of theory with the conductor-like polarizable continuum model (CPCM) for toluene.[6–10] To properly assign all stationary points as minima and saddle points, vibrational analysis was performed at the same level of theory as for geometry optimization. This analysis was also used for the Gibbs free energy corrections. Besides the vibrational analysis, the transition states were further confirmed through IRC calculations. Conformational analysis of the intermediates and transition states was performed with the CREST program and the best conformation was optimized at DFT level.[11] The TS1' energy was computed by using a relaxed scan using the dihedral angle H56N48C40C39 as the reaction coordinate. All attempts to fully optimize as a TS selected geometries from scan calculations using different reaction coordinates were unsuccessful. Since the TS1' is not involved in the rate-determining step, this approach was considered a good approximation. The non-covalent interaction figures were computed with the NCIplot program using the default options and an ultrafine grid.[12,13]

Imaginary frequencies for the transition states:

Transition State	Frequency
TSB1	678.5*i*
TSB2	652.0*i*
TSB3	662.4*i*
TSB4	665.5*i*
TSB5	633.9*i*
TSB6	634.8*i*
TSB7	681.0*i*
TSD1	63.1*i*
TSD2	679.8*i*
TSD3	645.5*i*
TSD4	643.4*i*
TSD5	668.6*i*

TSD6	653.1*i*
TSA1	658.3*i*
TSA2	927.8*i*
TSA3	561.0*i*
TSC1	683.1*i*

Table S2. Imaginary frequencies for the transition states.

Reported energies:

	G kcal mol^{-1}	H kcal mol^{-1}	E kcal mol^{-1}
OH^-	-47613.09975675	-47594.52317675	-47603.26236925
H_2O	-47960.3856785	-47939.751526	-47956.990206
BPA^-	-483262.99332825	-483188.19588575	-483395.08577325
Model A	-603976.5394085	-603882.6641535	-604146.2605885
Model B	-604717.28509375	-604625.15610125	-604904.84540125
Model C	-629359.99471975	-629261.49785725	-629557.88367725
Model D	-688727.65212625	-688623.24170375	-688955.47910875
B1	-652344.735329	-652246.5861015	-652534.5019265
B2	-652346.87353525	-652246.85937775	-652534.69049025
B3	-604381.5975055	-604290.267948	-604560.3106905
B4	-121129.7902505	-121096.7021055	-121157.561448
B5	-168767.4073035	-168729.697621	-168800.828511
B6	-169098.3967365	-169059.026689	-169140.2069915
B7	-168763.01680425	-168722.78024925	-168793.97890925
B8	-604382.21458175	-604289.65644925	-604559.60820425
TSB1	-652346.53242625	-652248.42837875	-652534.37448125
TSB2	-652320.63261475	-652217.75391975	-652505.15080225
TSB3	-604359.38720575	-604267.42512825	-604535.84641075
TSB4	-604359.49920725	-604264.40534725	-604532.75007475
TSB5	-168724.03732725	-168684.08809725	-168753.83597725
TSB6	-168723.1177815	-168681.443624	-168751.1908765
TSB7	-652307.58939975	-652208.41420975	-652496.87156725
D1	-736359.3116315	-736249.0158865	-736589.6944215
D2’	-736355.17948125	-736243.44487875	-736584.27150375
D3	-688396.10999125	-688292.53288875	-688614.53263125
D4	-205140.65143925	-205094.06639675	-205207.12997425
D5	-252777.561488	-252727.410363	-252850.855928

D6	-253107.26598925	-253054.79060425	-253188.23851925
D7	-688683.89359475	-688578.05065975	-688909.94984225
A1	-651593.173559	-651494.612064	-651768.1775915
A2	-651615.665167	-651518.4145195	-651792.4839295
A3	-651608.920225	-651507.5143425	-651781.417465
A4	-603635.5320635	-603542.849686	-603796.4180435
C1	-676966.6399415	-676862.2263815	-677171.5311715
C2	-676990.40455875	-676889.04002125	-677198.79221875
TSD1	-736352.28469825	-736244.79889825	-736584.76271075
TSD2	-736330.3319245	-736217.594577	-736557.412182
TSD3	-688373.92736425	-688268.80535675	-688589.57582675
TSD4	-252739.9239125	-252688.27118	-252810.180625
TSD5	-736319.16506	-736208.0642325	-736548.75218
TSD6	-688666.02615975	-688561.57941225	-688892.23175225
TSA1	-651572.06615325	-651474.60152825	-651747.18627325
TSA2	-651592.57629725	-651494.31544475	-651764.45419475
TSA3	-603579.76344025	-603533.37550275	-603768.91453025
TSC1	-676937.233158	-676833.7162955	-677141.6104655

	□G kcal mol^{-1}	□H kcal mol^{-1}
Model A + OH^-	0	0
A1	-5.4	-17.4
TSA1	15.7	2.6
A2	-27.9	-41.2

Table S3. Gibbs free energy and enthalpy for mechanism SN model A, the intermediaries and TS are anionic.

	ΔG kcal mol^{-1}	ΔH kcal mol^{-1}
Model B + OH^-	0	0
B1	-14.4	-26.9
TSB7	22.8	11.3
B6 + $BPAO^-$	-31.0	-27.5

Table S4. Gibbs free energy and enthalpy for mechanism SN model B.

	ΔG kcal mol^{-1}	ΔH kcal mol^{-1}
Model C + OH^-	0	0
C1	6.5	-6.2
TSC1	35.9	22.3
C2	-31.0	-27.5

Table S5. Gibbs free energy and enthalpy for mechanism SN model C.

	ΔG kcal mol^{-1}	ΔH kcal mol^{-1}
Model D + OH^-	0	0
D1	-18.6	-31.3
TSD5	21.6	41.0
D6 + $BPAO^-$	-29.5	-25.2

Table S6. Gibbs free energy and enthalpy for mechanism SN model D.

	ΔG kcal mol^{-1}	ΔH kcal mol^{-1}
Model A + OH^-	0	0
A1	-3.5	-17.4
TSA2	-1.0	-17.1
A3	-17.4	-30.2
TSA3 + H_2O	49.5	4.1
A4 + H_2O	-6.3	-5.4

Table S7. Gibbs free energy and enthalpy for mechanism cyclopropenone mechanism.

	ΔG kcal mol^{-1}	ΔH kcal mol^{-1}
Model D	0	0
TSD6	63.5	61.7
D9	45.7	45.2

Table S8. Gibbs free energy and enthalpy for amine as base.

	ΔG kcal mol^{-1}	ΔH kcal mol^{-1}
Model B + 2 x OH^-	0	0
B1 + OH^-	-14.4	-26.9
TSB1 + OH^-	-16.1	-28.7
B2 + OH^-	-16.5	-27.2
B3 + H_2O + OH^-	-11.6	-10.3
TSB3 + H_2O + OH^-	10.6	12.5
B4 + $BPAO^-$ + H_2O + OH^-	-22.8	-5.0
TSB4 + $BPAO^-$ + H_2O	-3.9	2.2
B5 + $BPAO^-$ + H_2O	-47.3	-43.4

Table S9. Gibbs free energy and enthalpy for mechanism epoxide closure Model 2.

	ΔG kcal mol^{-1}	ΔH kcal mol^{-1}
Model B + 2 x OH^-	0	0
B1 + OH^-	-14.4	-26.9
TSB1 + OH^-	-16.1	-28.7
B2 + OH^-	-16.5	-27.2
TSB2 + OH^-	9.8	1.9
B4 + $BPAO^-$ + H_2O + OH^-	-22.8	-5.0
TSB4 + $BPAO^-$ + H_2O	-3.9	2.2
B5 + $BPAO^-$ + H_2O	-47.3	-43.4

Table S10. Gibbs free energy and enthalpy for mechanism epoxide closure Model 2 with TSB2.

	ΔG kcal mol^{-1}	ΔH kcal mol^{-1}
Model D + 2 x OH^-	0	0
D1 + OH^-	-18.6	-31.3
TSD1 + OH^-	-11.5	-27.0
D2 + OH^-	-14.4	-25.7
D3 + H_2O + OH^-	-15.7	-14.5
TSD3 + H_2O + OH^-	6.4	9.2
D4 + $BPAO^-$ + H_2O + OH^-	-23.3	-4.2
TSD4 + $BPAO^-$ + H_2O	-9.5	-3.9
D5 + $BPAO^-$ + H_2O	-47.1	-43.1

Table S11. Gibbs free energy and enthalpy for mechanism epoxide closure Model 4.

	ΔG kcal mol^{-1}	ΔH kcal mol^{-1}
Model D + 2 x OH^-	0	0
D1 + OH^-	-18.6	-31.3
TSD1 + OH^-	-11.5	-27.0
D2 + OH^-	-14.4	-25.7
TSD2 + OH^-	10.4	0.2
D4 + $BPAO^-$ + H_2O + OH^-	-23.3	-4.2
TSD4 + $BPAO^-$ + H_2O	-9.5	-3.9
D5 + $BPAO^-$ + H_2O	-47.1	-43.1

Table S12. Gibbs free energy and enthalpy for mechanism epoxide closure Model 4 with TS2'.

	ΔG kcal mol^{-1}	ΔH kcal mol^{-1}
B4 + OH^-	0	0
TSB4	20.8	14.1
B5	-22.6	-31.5

Table S13. Gibbs free energy and enthalpy for B4 opening with hydroxide position 1.

	ΔG kcal mol^{-1}	ΔH kcal mol^{-1}
B4 + OH^-	0	0
TSB6	23.3	15.6
B7	-16.6	-25.7

Table S14. Gibbs free energy and enthalpy for B4 opening with hydroxide position 2.

	ΔG kcal mol^{-1}	ΔH kcal mol^{-1}
B4 + $BPAO^-$	0	0
TSB3	33.4	17.5
B3	11.2	-5.4

Table S15. Gibbs free energy and enthalpy for B4 opening with BPAO- position 1.

	ΔG kcal mol^{-1}	ΔH kcal mol^{-1}
B4 + $BPAO^-$	0	0
TSB4	35.2	20.5
B8	12.5	-4.8

Table S16. Gibbs free energy and enthalpy for B4 opening with BPAO- position 2.

Intrinsic reaction coordinate (IRC):

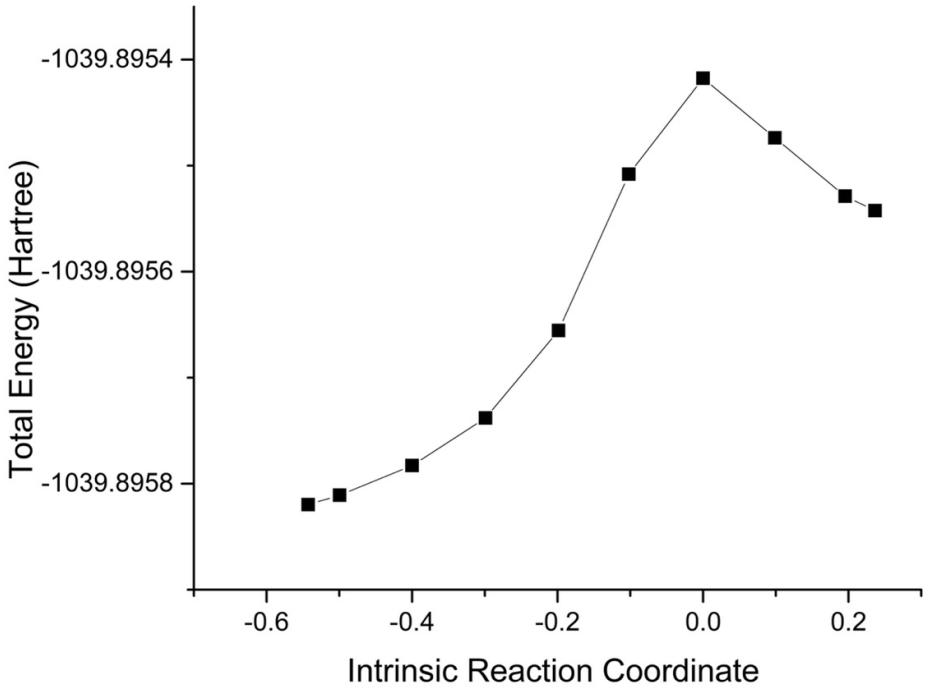

Figure S13. IRC calculation for TSB1.

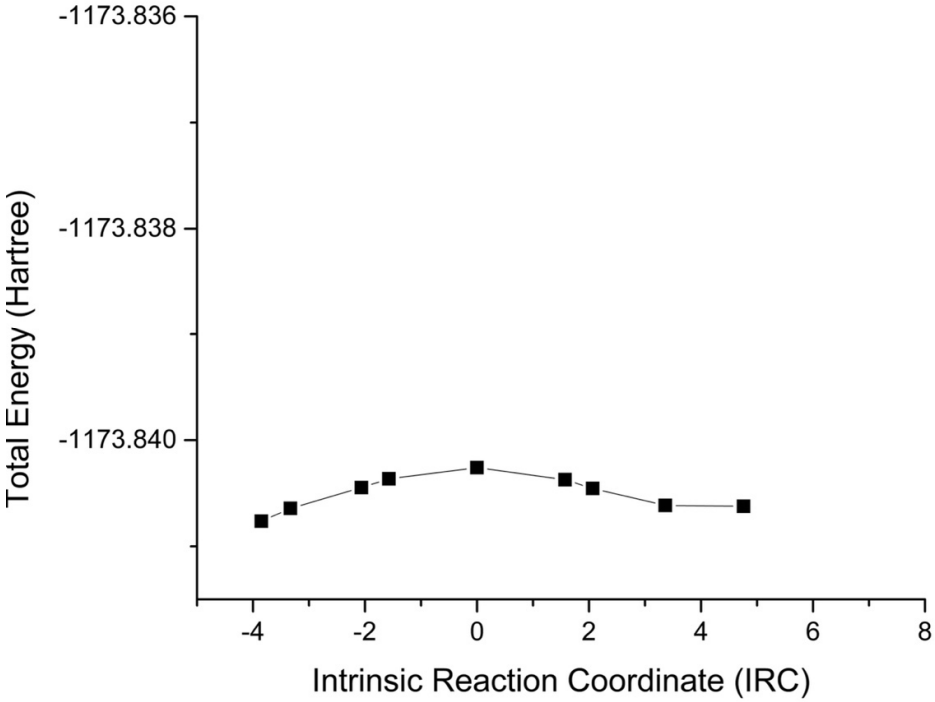

Figure S14. IRC calculation for TSD1.

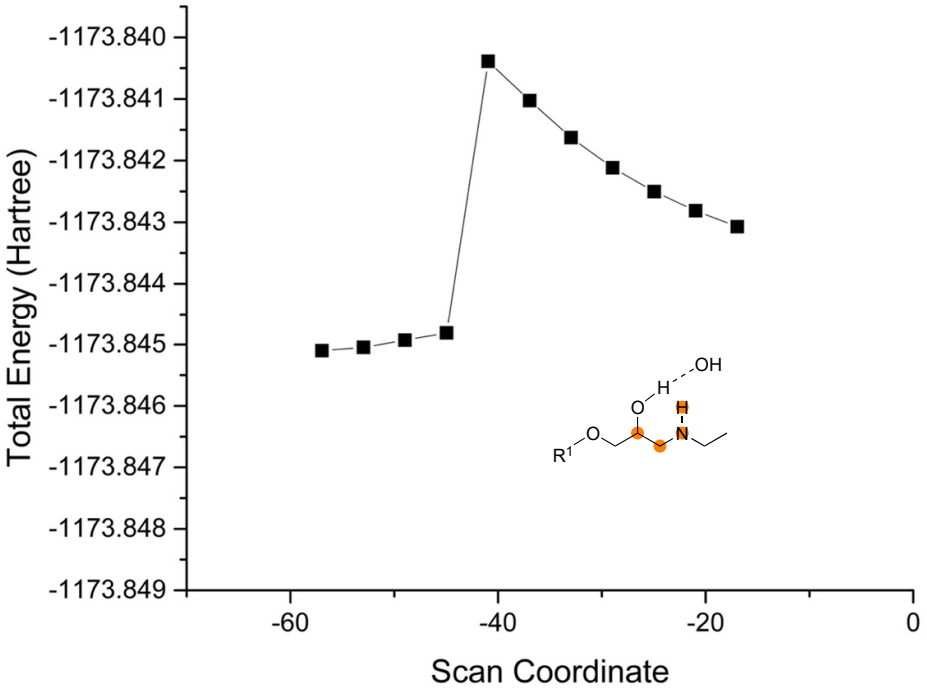

Figure S15. Scan calculation for TSD1 (H56N48C40C39 – marked in orange).

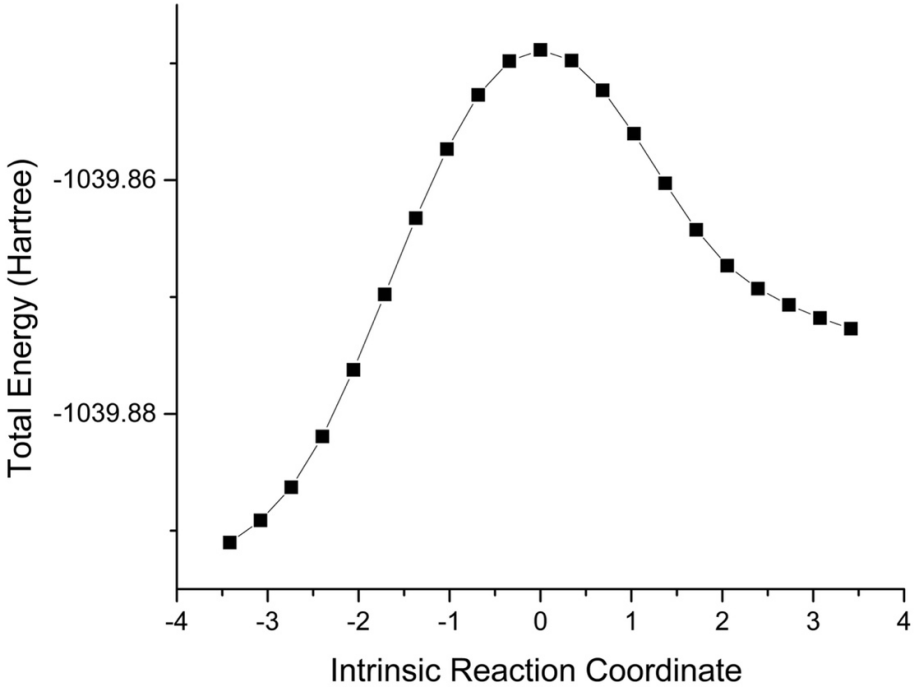

Figure S16. IRC calculation for TSB2.

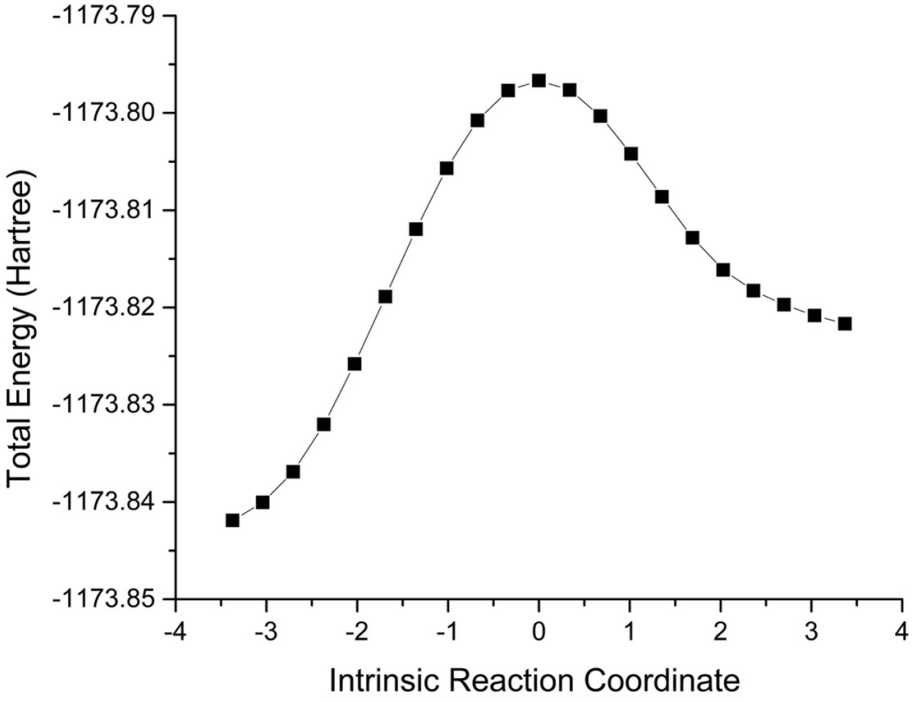

Figure S17. IRC calculation for TSD2.

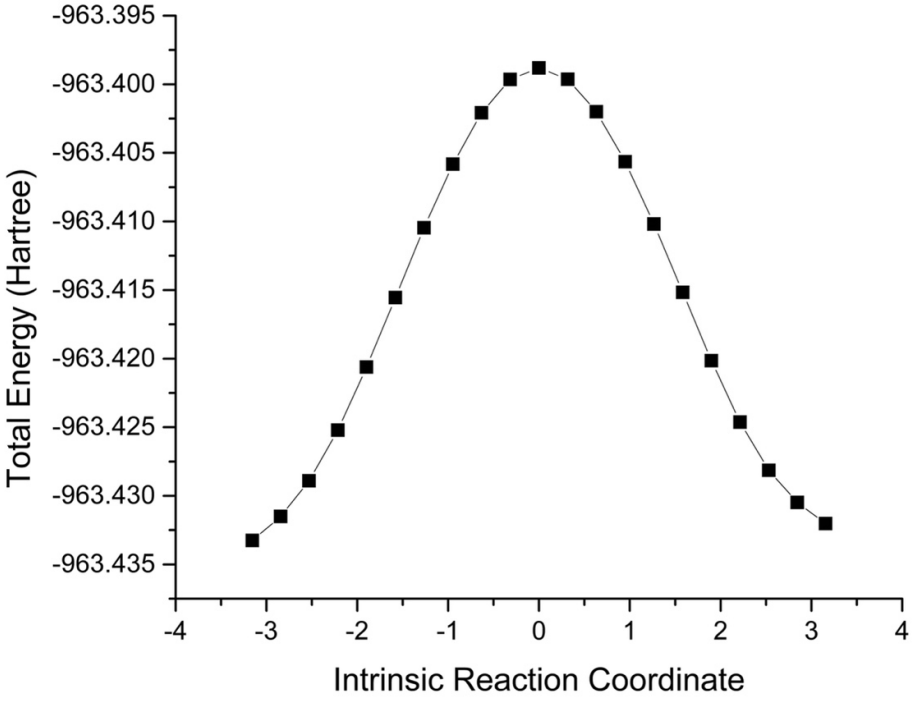

Figure S18. IRC calculation for TSB3.

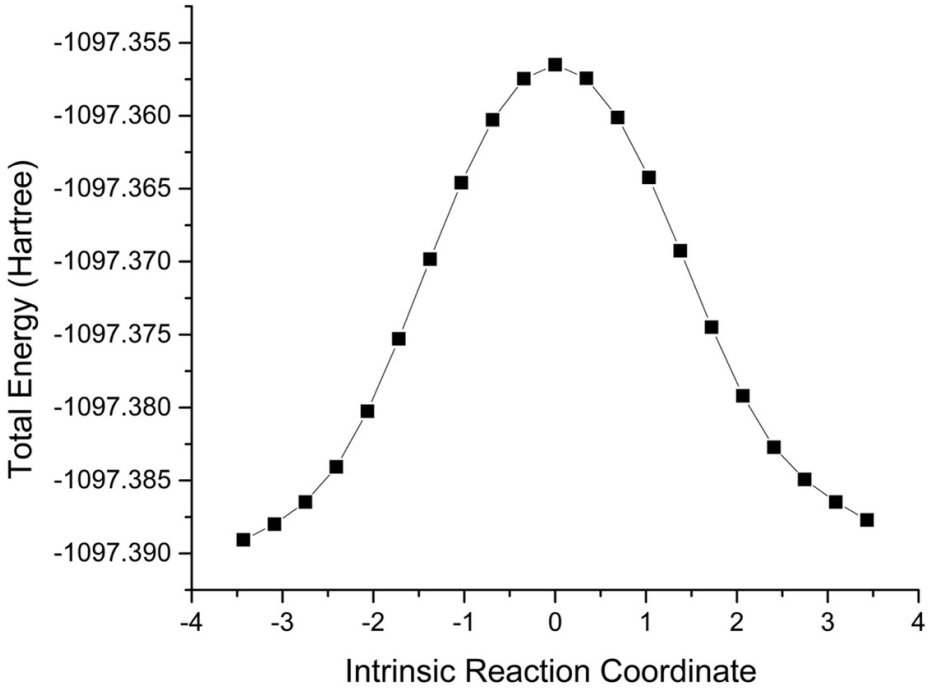

Figure S19. IRC calculation for TSD3.

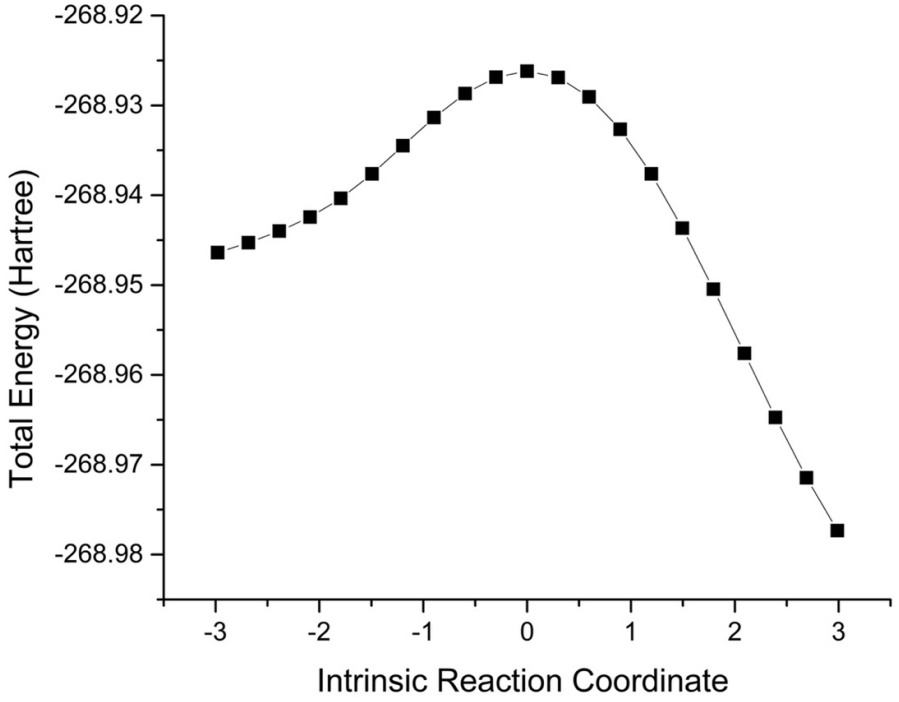

Figure S20. IRC calculation for TSB4.

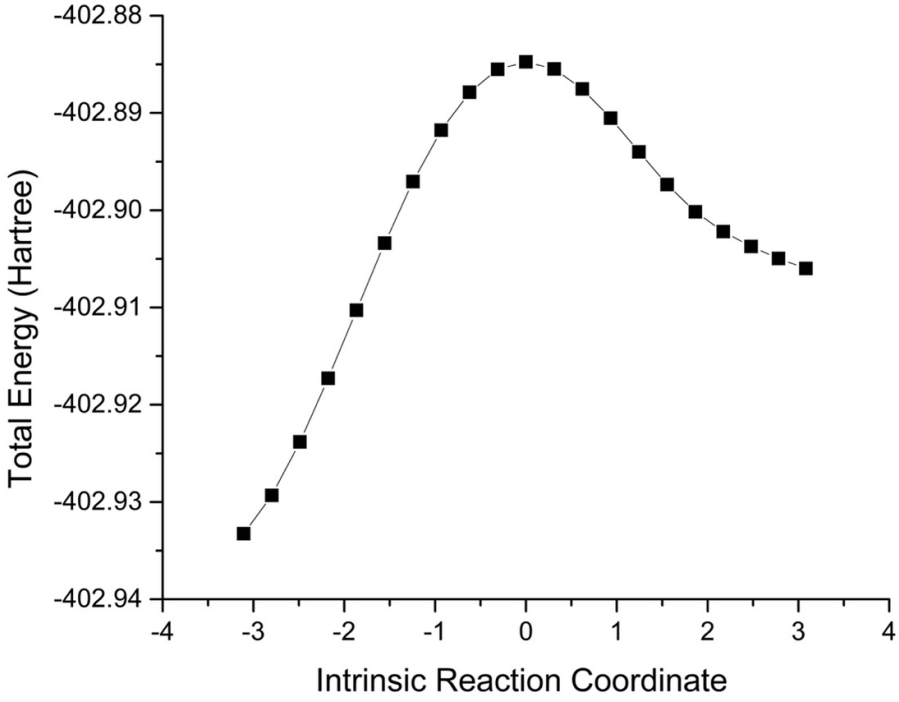

Figure S21. IRC calculation for TSD4.

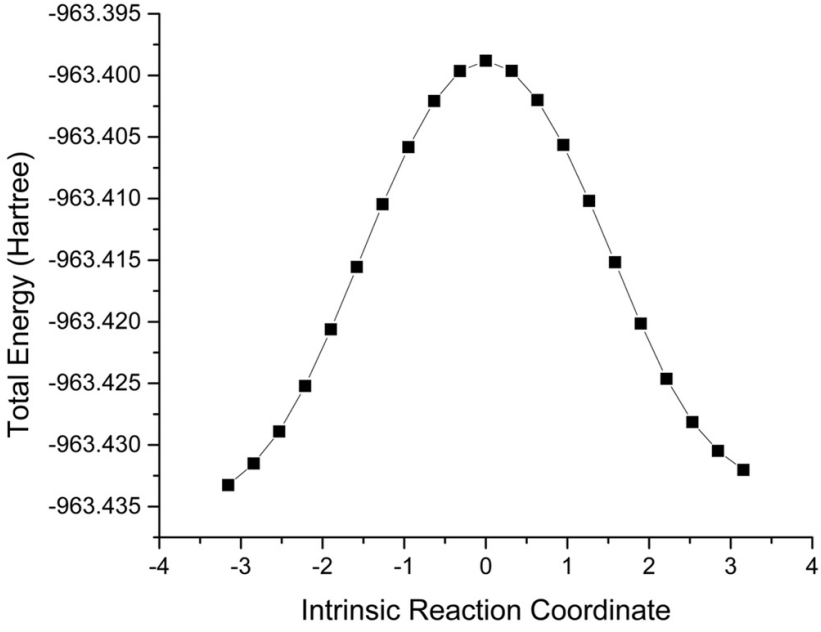

Figure S22. IRC calculation for TSB5.

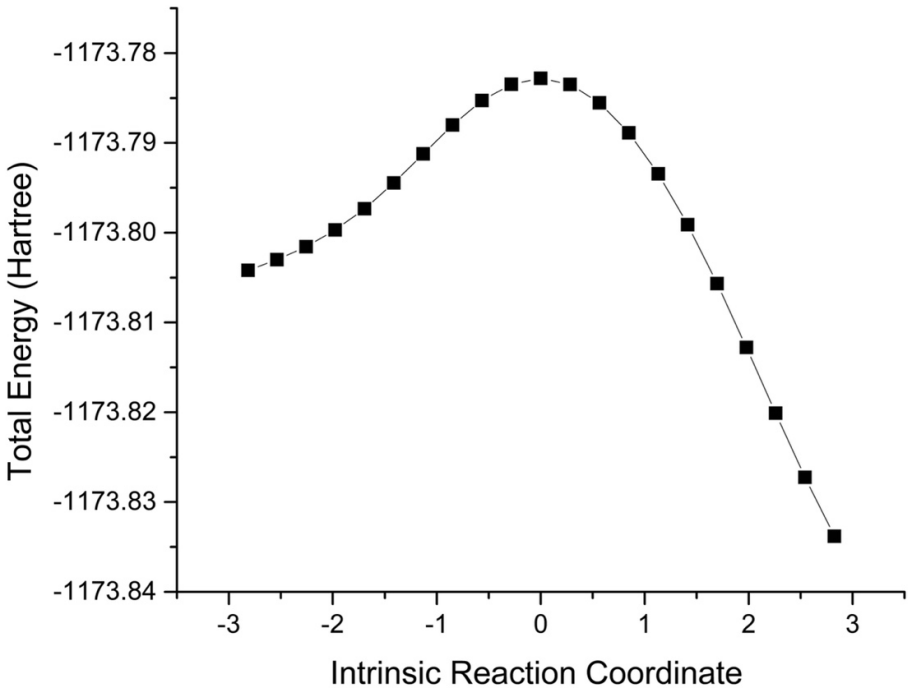

Figure S23. IRC calculation for TSD5.

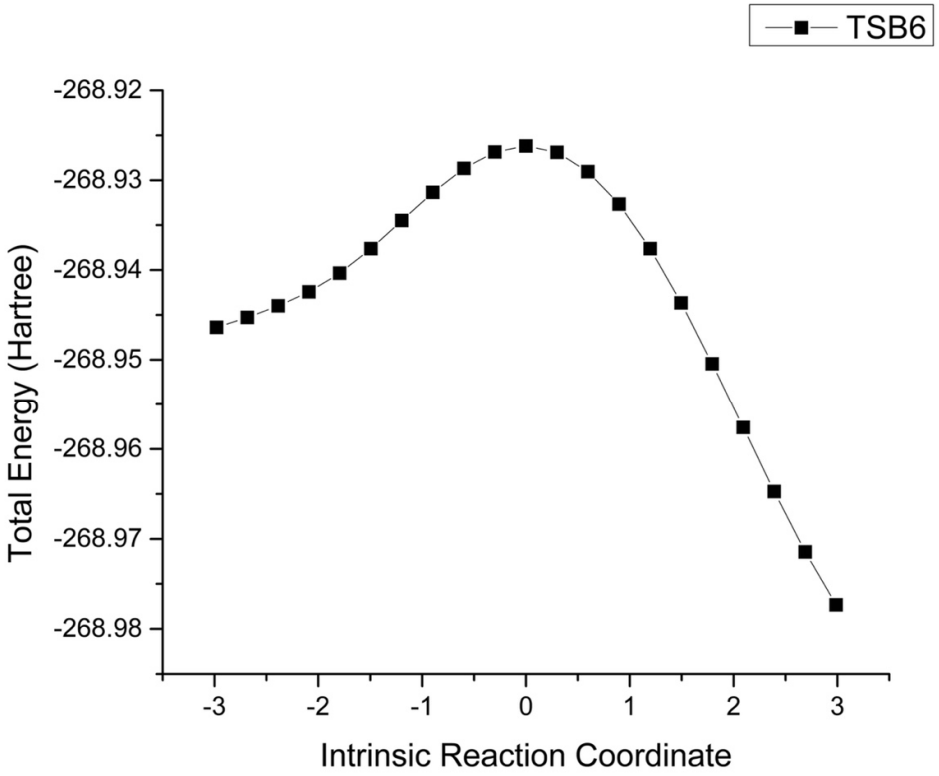

Figure S24. IRC calculation for TSB6.

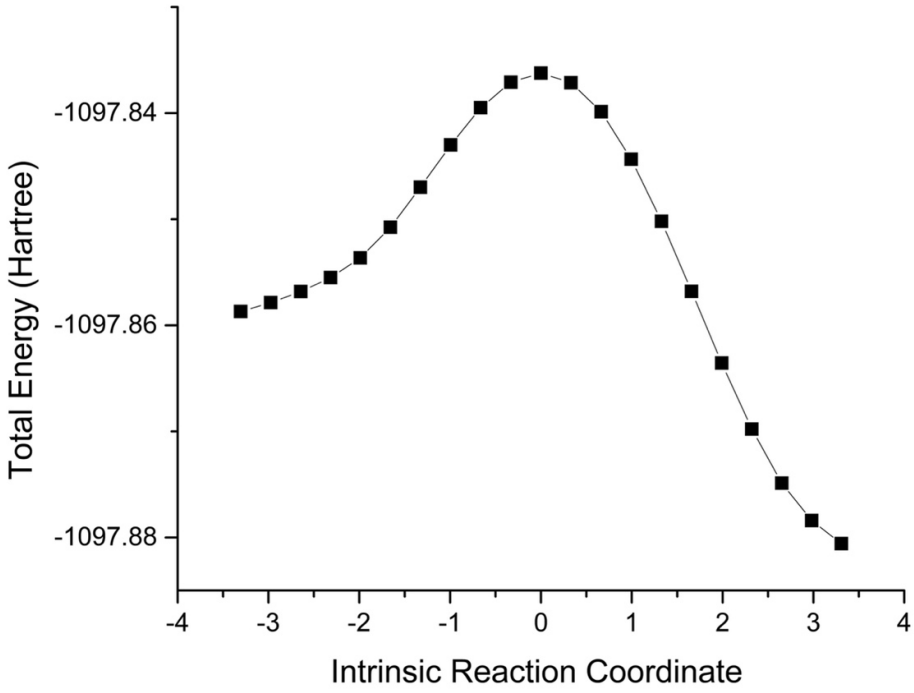

Figure S25. IRC calculation for TSD6.

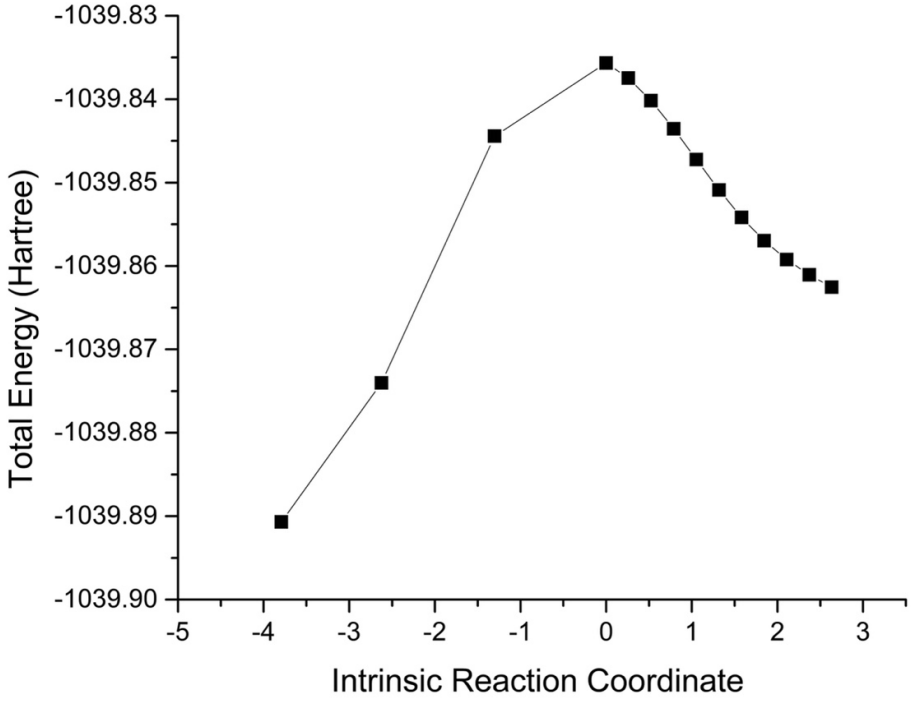

Figure S26. IRC calculation for TSB7.

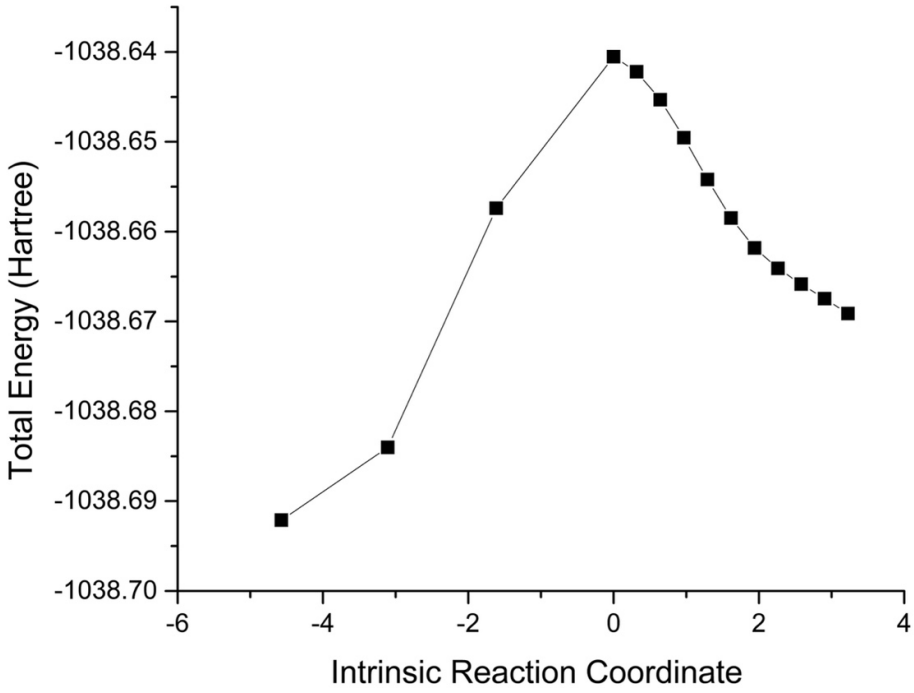

Figure S27. IRC calculation for TSA1.

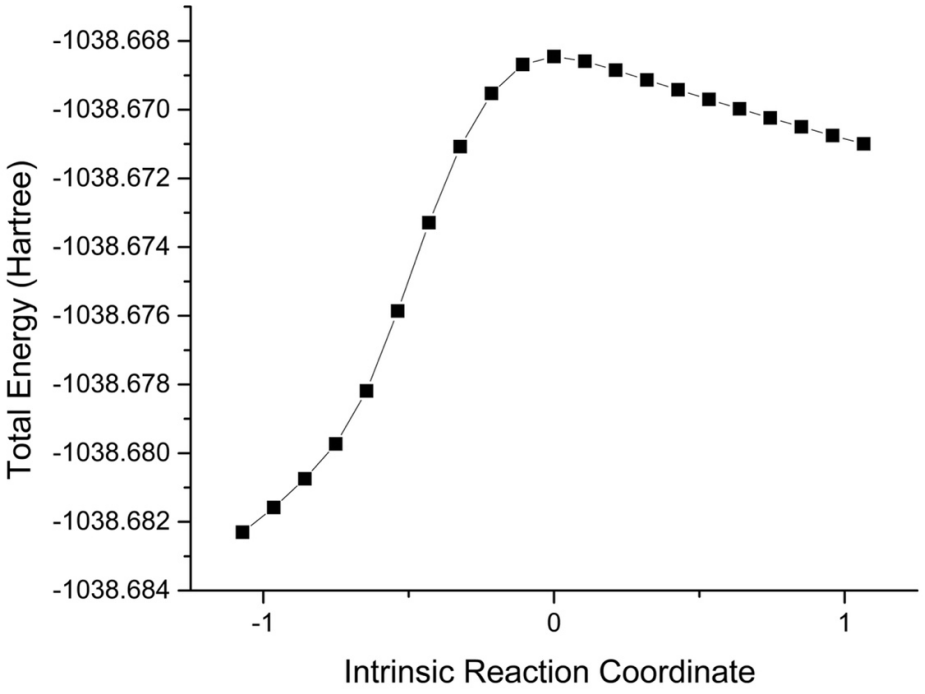

Figure S28. IRC calculation for TSA2.

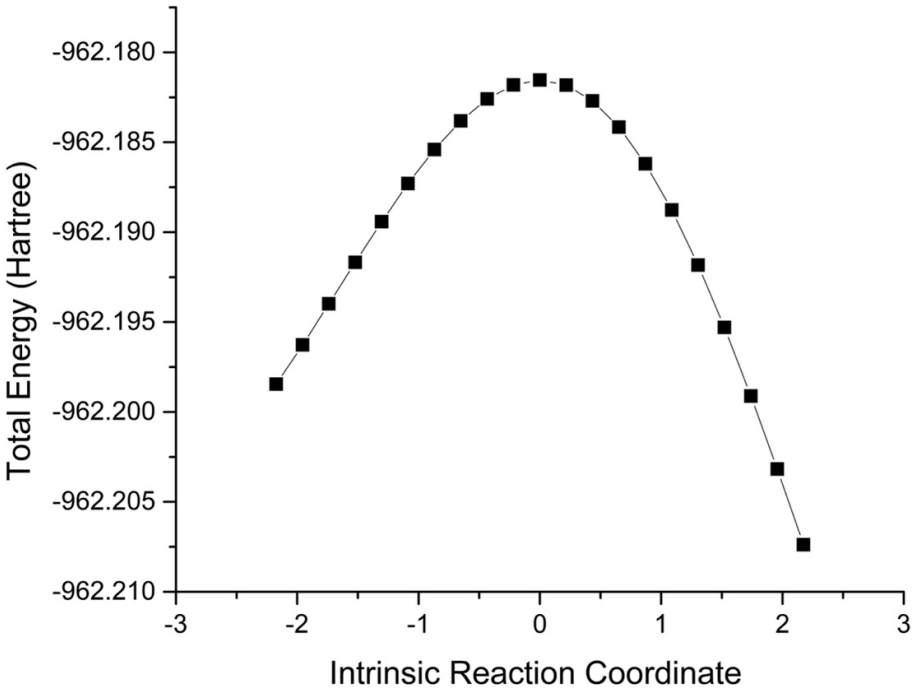

Figure S29. IRC calculation for TSA3.

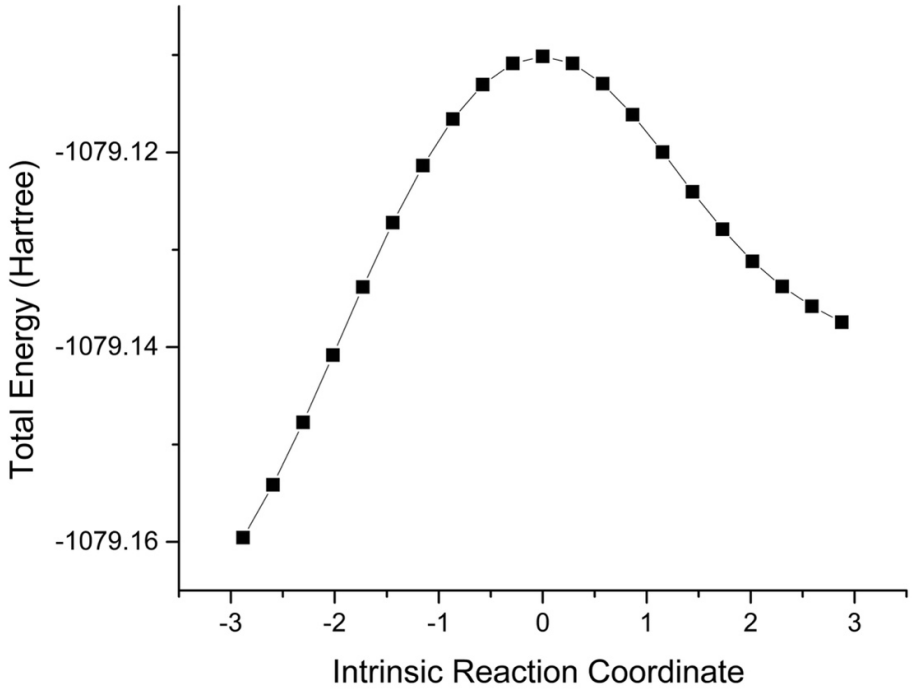

Figure S30. IRC calculation for TSC1.

5. References

1 Henriksen, M. L., Friis, J. E., Voss, A. & Hinge, M. Recyclable carbon fibre composites enabled by cystine containing epoxy matrices. *RSC Adv.* **9**, 31378-31385 (2019).

2 Ahrens, A., Bonde, A., Sun, H., Wittig, N. K., Hammershøj, H. C. D., Batista, G. M. F., Sommerfeldt, A., Frølich, S., Birkedal, H. & Skrydstrup, T. Catalytic disconnection of C–O bonds in epoxy resins and composites. *Nature* **617**, 730-737 (2023).

3 Hanada, S., Yuasa, A., Kuroiwa, H., Motoyama, Y. & Nagashima, H. Hydrosilanes Are Not Always Reducing Agents for Carbonyl Compounds, II: Ruthenium-Catalyzed Deprotection of tert-Butyl Groups in Carbamates, Carbonates, Esters, and Ethers. *Eur. J. Org. Chem.* **2010**, 1021-1025 (2010).

4 Pan, W., Li, C., Zhu, H., Li, F., Li, T. & Zhao, W. A mild and practical method for deprotection of aryl methyl/benzyl/allyl ethers with HPPh2 and tBuOK. *Org. Biomol. Chem.* **19**, 7633-7640 (2021).

5. Frisch, M. J.; Trucks, G. W.; Schlegel, H. B.; Scuseria, G. E.; Robb, M. A.; Cheeseman, J. R.; Scalmani, G.; Barone, V.; Petersson, G. A.; Nakatsuji, H.; Li, X.; Caricato, M.; Marenich, A. V.; Bloino, J.; Janesko, B. G.; Gomperts, R.; Mennucci, B.; Hratch, D. J. Gaussian 16, Revision B.01. at (2016).

6. Zhao, Y. & Truhlar, D. G. The M06 suite of density functionals for main group thermochemistry, thermochemical kinetics, noncovalent interactions, excited states, and transition elements: two new functionals and systematic testing of four M06-class functionals and 12 other function. *Theor. Chem. Acc.* **120**, 215–241 (2008).

7. Barone, V. & Cossi, M. Quantum Calculation of Molecular Energies and Energy Gradients in Solution by a Conductor Solvent Model. *J. Phys. Chem. A* **102**, 1995–2001 (1998).

8. McLean, A. D. & Chandler, G. S. Contracted Gaussian basis sets for molecular calculations. I. Second row atoms, Z =11–18. *J. Chem. Phys*. **72**, 5639–5648 (1980).

9. Krishnan, R., Binkley, J. S., Seeger, R. & Pople, J. A. Self-consistent molecular orbital methods. XX. A basis set for correlated wave functions. *J. Chem. Phys.* **72**, 650–654 (1980).

10. Blaudeau, J.-P., McGrath, M. P., Curtiss, L. A. & Radom, L. Extension of Gaussian-2 (G2) theory to molecules containing third-row atoms K and Ca. *J. Chem. Phys*. **107**, 5016–5021 (1997).

11. Pracht, P., Bohle, F. & Grimme, S. Automated exploration of the low-energy chemical space with fast quantum chemical methods. *Phys. Chem. Chem. Phys*. **22**, 7169–7192 (2020).

12. Contreras-García, J. et al. NCIPLOT: A Program for Plotting Noncovalent Interaction Regions. *J. Chem. Theory Comput*. **7**, 625–632 (2011).

13. Johnson, E. R. et al. Revealing Noncovalent Interactions. *J. Am. Chem. Soc*. **132**, 6498–6506 (2010).